THE DESIGN AND APPLICATION OF AN AUTOMATED LUMINOMETER FOR CHEMILUMINESCENCE

by

Ian Chapple

Dissertation submitted to the Faculty of the
Virginia Polytechnic Institute and State University
in partial fulfillment of the requirements
for the degree of
DOCTOR OF PHILOSOPHY
in
Chemistry

APPROVED:

R. E. Dessy, Chairman

H. M. McNair

J. G. Mason

J. F. Wolf

J. E. McGrath

November, 1984

Blacksburg, Virginia

To

for her love and patience

ACKNOWLEDGEMENTS

The person to whom I am most deeply indebted for this work is my mother . If it were not for her initial faith in my abilities and continued support, my venture into tertiary education would never have started, nor would it have been seen through to completion.

I would like to thank Dr. and Dr. Harold McNair for offering me the initial opportunity to come to the United States to attend graduate school. Also special thanks goes to Dr. and family for providing a familiar face and a familiar accent during those first few months of adjustment.

Thanks also goes to Dr. Ray Dessy for providing an environment in which so many talented people have congregated and shared their skills. The members of the Laboratory Automation and Instrument Design group have been a constant source of knowledge, inspiration and friendship for which I will always be grateful. In particular I must thank , without whose help and advice, on such subjects as biochemistry and pulse counting, this particular project would never have come to completion.

Finally, I would like to thank my wife for constantly providing me with the inspiration to go on and with the notion that, yes, there is life after

graduate school.

Table of Contents

List of Figures

Figure page

List of Tables

INTRODUCTION

Chemiluminescence can be defined as the generation of electronically excited states by means of a chemical reaction and the subsequent dissipation of this electronic energy in the form of fluorescence. The known chemiluminescing reactions are many and varied, as are the structures of the luminescing species. Chemiluminescence has been observed from the reaction of simple gases, aromatic hydrocarbons and biological molecules.

This diversity would imply that there is no single common mechanism associated with a chemiluminescent process. Hercules has stated that the requirements for an efficient chemiluminescent process are: "sufficient excitation energy; presence of a species capable of forming an electronically excited state; an emitter to give off the excitation energy; a fast reaction rate and a reaction coordinate system that is favorable to excited state production" (1). The energy available from most chemiluminescent reactions is sufficient for the excitation of large aromatic molecules. It is, therefore, not surprising that the vast majority of these reactions involve large molecules with low lying antibonding orbitals and high fluorescence efficiencies.

The use of chemiluminescence as an analytical tool became truly viable with Albrechts' discovery of

"luminol", 5-amino-2,3-dihydrophthalazine-1,4-dione, which is a simple, easy to handle molecule that can be produced in high purity and which has one of the highest chemiluminescent efficiencies known for a non-biological molecule (2). The chemiluminescent efficiency of a reaction is define as:

$$\text{eff.} = \frac{\text{einsteins of light produced}}{\text{moles of reactant consumed}} \qquad [1]$$

The efficiency of the luminol reaction is about 0.01 whereas some biological systems such as the firefly reaction have efficiencies approaching unity (3).

From an instrumental standpoint, chemiluminescence shares many of the desirable characteristics of fluorescence. With chemiluminescence, one measures a small signal against an essentially zero background, as opposed to trying to observe a small decrease in a very large background as is the case with absorption. This feature eliminates the need for dual beam instrumentation and synchronous detection systems. In chemiluminescence the exciting reaction is fairly specific, which usually results in a single emitting species, therefore, there is little need to discriminate wavelengths. This eliminates the need for an emission monochromator, which not only simplifies the instrumentation but also increases the

overall light throughput to the detector. As a result chemiluminescent instrumentation tends to be simple, inexpensive and yet capable of very good sensitivity.

The luminol reaction can regularly achieve detection limits in the 10^{-9} to 10^{-10}M range when analyzing for metal ions such as Fe(II) and Cr(III) and oxidants such as H_2O_2 and OCl^- (3). The firefly reaction, which is most often used for the determination of ATP, has been able to detect concentrations of ATP in the $1x10^{-12}$M to $1x10^{-11}$M range (3).

One of the major disadvantages of chemiluminescent analyses, especially with luminol, has been low selectivity. In an attempt to overcome this problem chemilumin1ent reactions have been used as a detector for much more specific reactions, namely various enzyme reactions. With the mating of two such reactions one still maintains the instrumental simplicity and sensitivity of traditional chemiluminescence and gains the considerable selectivity of the enzyme for its substrate. The bioluminescent reactions, such as that of the firefly, are naturally enzyme/substrate reactions and already possess an inherent selectivity.

Because a large number of these biochemical reactions, which can be followed by chemiluminescence, are also of considerable clinical importance, it is in this

field that most of the active research on chemiluminescent analysis is taking place.

Radio immunoassay is an important clinical technique, however, this method is receiving considerable criticism due to its environmental and safety impact. Various substitutes for this technique have been suggested, fluorescence immunoassay being the one most well developed. However, chemiluminescence immunoassay is actively being studied as a more sensitive alternative to the fluorescence technique (4).

An interesting alternative use of chemiluminescence suggested by Freeman and Seitz was the immobilization of a chemiluminescent system on to the end of a fiber optic bundle to yield a substrate specific optical probe which could be used in much the same way as an ion specific electrode (5). Before such a device could ever be made practical, a chemiluminescent system would have to be found that does not destroy the luminescing reagent, so that a constant fresh supply of this reagent was not necessary.

Cilento et. al. described a biochemical reaction which is luminescent and which appears to regenerate the luminescing species (6). If this is indeed the case it may serve as a starting point in the development of an optical probe similar to that proposed by Freeman and

Seitz. In this light, the goal of this research is to investigate the reaction described by Cilento to determine if the luminescing species is indeed recycling and if so to determine the analytical applicability of the reaction.

HISTORICAL

In 1928 H. O. Albrecht discovered that strong chemiluminescence could be obtained from certain cyclohydrazides in alkaline solution in the presence of various oxidizing agents (2). The most notable of these was 3-aminophthalic hydrazide, which could yield visible luminescence at concentrations as low as 10^{-8}M when both hydrogen peroxide and ferricyanide were included. Because of its uniquely high quantum efficiency this particular molecule received considerable attention, and it quickly developed the common name of "luminol". Luminol still remains, even today, one of the most efficient chemiluminescing molecules, outside of a few of the naturally occurring bioluminescent compounds.

Since Albrecht's time the reactions of luminol have been studied extensively and a large number of analytical applications have been developed around them. Each one of the basic components of the luminol reaction:

$$\text{luminol} + H_2O_2 \xrightarrow{M^{n+}} \text{3-aminophthalic acid} + N_2 + \text{light} \quad [2]$$

has been exploited for analytical purposes. It has been discovered that there are a considerable number of transition metals, such as Cu, Fe, Co and Cr, which can be used to catalyze this reaction. By maintaining an excess

of the other reagents, it has been found that the light intensity is proportional to the metal ion concentration. While the luminol reaction provides a very simple, sensitive method for the determination of these metals it lacks the selectivity needed for such things as ground water samples.

A number of unique solutions to this problem have been employed in order to make the luminol reaction a viable tool. Seitz, Suydam and Hercules described a technique for the quantitation of Cr(III) which relied upon the fact that the rate of complexing with EDTA was considerably slower for Cr(III) than for the other interfering ions (7). Another analytical scheme, also described by Seitz and Hercules, relied upon the fact that chemiluminescence could be catalyzed by Fe(II) in the absence of H_2O_2 (8). In this particular instance dissolved oxygen acted as the oxidant. This concept has been extended to the quantitation of hemoglobin and other hemoproteins in serum samples (9).

Another avenue of active investigation has been the use of the luminol reaction for the determination of oxidants, in particular H_2O_2. A continuous flow system for the determination of H_2O_2 in natural water has been based on an excess of luminol and potassium ferricyanide as the catalyst (10). This particular device could

routinely determine concentrations of hydrogen peroxide down to 6×10^{-7}M.

Some of the most promising work, utilizing the detection of H_2O_2, has been in the area of indirect determinations. That is, to use the luminol reaction as a sensor for hydrogen peroxide, which itself is the product of some other primary reaction. The most successful applications of this concept have been with biochemical reactions where an enzyme/substrate reaction yields H_2O_2. A widely studied example has been the determination of glucose with glucose oxidase.

$$\text{glucose} + O_2 + H_2O \xrightarrow[\text{oxidase}]{\text{glucose}} \text{gluconic acid} + H_2O_2 \quad [3]$$

$$\text{luminol} + H_2O_2 \xrightarrow{Fe(CN)_6^{3-}} \text{3-aminophthalic acid} + N_2 + \text{light} \quad [4]$$

The coupling of the luminol reaction to biochemical reactions introduces another series of logistic problems. The most important of these is a mismatch in the optimum pH for the two consecutive reactions. Most of the biochemical reactions have pH optima around pH 7 while the luminol reaction runs most efficiently in the pH 11-12 range. Auses, Cook and Maloy overcame this problem by employing a pH jump technique (11). In their system the glucose was oxidized in an unbuffered, pH 7,

enzyme/luminol solution. At measurement time this solution was then mixed with a strongly buffered $Fe(CN)_6^{3-}$ solution. This technique was carried one step further by Bobstick and Hercules (12). Here a continuous flow system was designed where the glucose sample was carried through a column of immobilized glucose oxidase and the effluent was mixed with a luminol/$Fe(CN)_6^{3-}$ stream in front of the detector. This particular system gave excellent results for glucose concentrations in the range of 10^{-8}M to 10^{-4}M.

A totally different approach to the application of coupled chemiluminescent reactions has been to carry them out, not entirely in solution, but at a solid liquid interface. These interfaces have taken various forms including filtration gels, hydrated membranes and glass rods (13,14,15). In almost all cases they involve the immobilization of one or more enzymes onto the solid surface and applying an analyte solution.

Lippman has described a solid-phase chemiluminescent system for the analysis of thiols (16). His technique entailed the covalent binding of a derivatized luminol to a polysaccharide by means of a disulphide bridge. When a sample solution containing another thiol or other strong nucleophile was eluted through the polysaccharide a sulphide exchange reaction would take place, releasing the bound luminol. The eluted luminol would then be mixed

with H_2O_2 and ferricyanide to yield the chemiluminescence.

Ikariyama, Aizawa and Suzuki demonstrated luminous membranes which consisted of an inert protein, such as albumin, cross linked with glutaraldehyde (14). Both glucose oxidase and peroxidase were also co-immobilized in this membrane. When an aqueous solution of glucose and luminol was applied, chemiluminescence could be detected at the membrane surface. The membrane concept has been extended by Vogelhut to a fully self-contained analytical unit employing the enzymes to produce H_2O_2, a chemiluminescent reagent such as luminol, peroxidase to catalyze the chemiluminescent reaction and a photosensitive detector layer (17).

An alternative to the membrane idea has been to immobilize the luminescence generating enzymes on the end of a light guide such as a glass rod or fiber optic bundle. Lee, Jablonski and DeLuca immobilized firefly luciferase to glass beads which were then cemented to the end of glass rods (15). These rods would then be dipped into a cell containing ATP, luciferase and Mg^{2+} ions to yield chemiluminescence which was proportional to the ATP concentration. Freeman and Seitz, on the other hand, immobilized peroxidase and luminol in a polyacrylamide gel which they held to the end of a fiber optic bundle by means of a fine nylon mesh (5). When this probe was

dipped into a beaker containing H_2O_2 a steady state signal proportional to peroxide concentration was observed. The main limitation encountered with this detector was the depletion of luminol at the reaction site. To compensate somewhat for this depletion, luminol had to be added to each sample solution.

One common characteristic of all the previously described chemiluminescent applications is that the actual luminescing reagent was not reuseable. While this may not be an important criterion for some of the applications, it would be highly desirable in such instances as the luminous membranes and light guide detectors. Ideally, one would like a luminescent reaction in which the luminescing species would be left intact after emission so that it could be reexcited by another analyte molecule. The type of reaction which comes to mind is that of a reversible electron transfer where the luminescent species is first oxidized and subsequently reduced, but where the reduced form is electronically excited and then fluoresces.

Cilento et. al. described observing luminescence from the oxidation of NADH by peroxidase when using eosin as the catalyzing phenol (6). It has been known from the early 1960's that this oxidation could be accelerated by the addition of certain phenols (18,19,20). Cilento's

group postulated that if a large conjugated phenol, such as eosin, were used, they might affect electron transfer into an unoccupied molecular orbital which would result in subsequent fluorescence. If this is indeed happening, the reaction would satisfy the basic requirement for a reuseable luminescing species.

INSTRUMENTATION

Manual Luminometer

The initial luminometer design was a relatively simple one, built along the lines of that described by Arrio et. al. (21). It is illustrated in figure 1. The instrument consists of a sealed aluminum box with an exterior, end on photomultiplier housing mounted flush with a 1 inch diameter hole cut in the end of the box. A four inch square hole was cut in the top of the box to provide access to the interior. This hole was sealed with the cell compartment cover from a Heath EU-701 UV/Visible spectrometer.

A manually operated shutter, again from the Heath EU-701, was interposed between the detector and the cell holder. The state of the shutter could be sensed by means of a microswitch which was positioned to close whenever the shutter was opened. The cell consisted of a 10 mm x 75 mm glass test tube which was secured to the shutter housing by a machined plastic block. Sample injections were made with a manually operated syringe through a short length of 1 mm teflon tubing which was brought to the exterior of the box by means of a chassis mounted Luer fitting. While this luminometer design suffered from

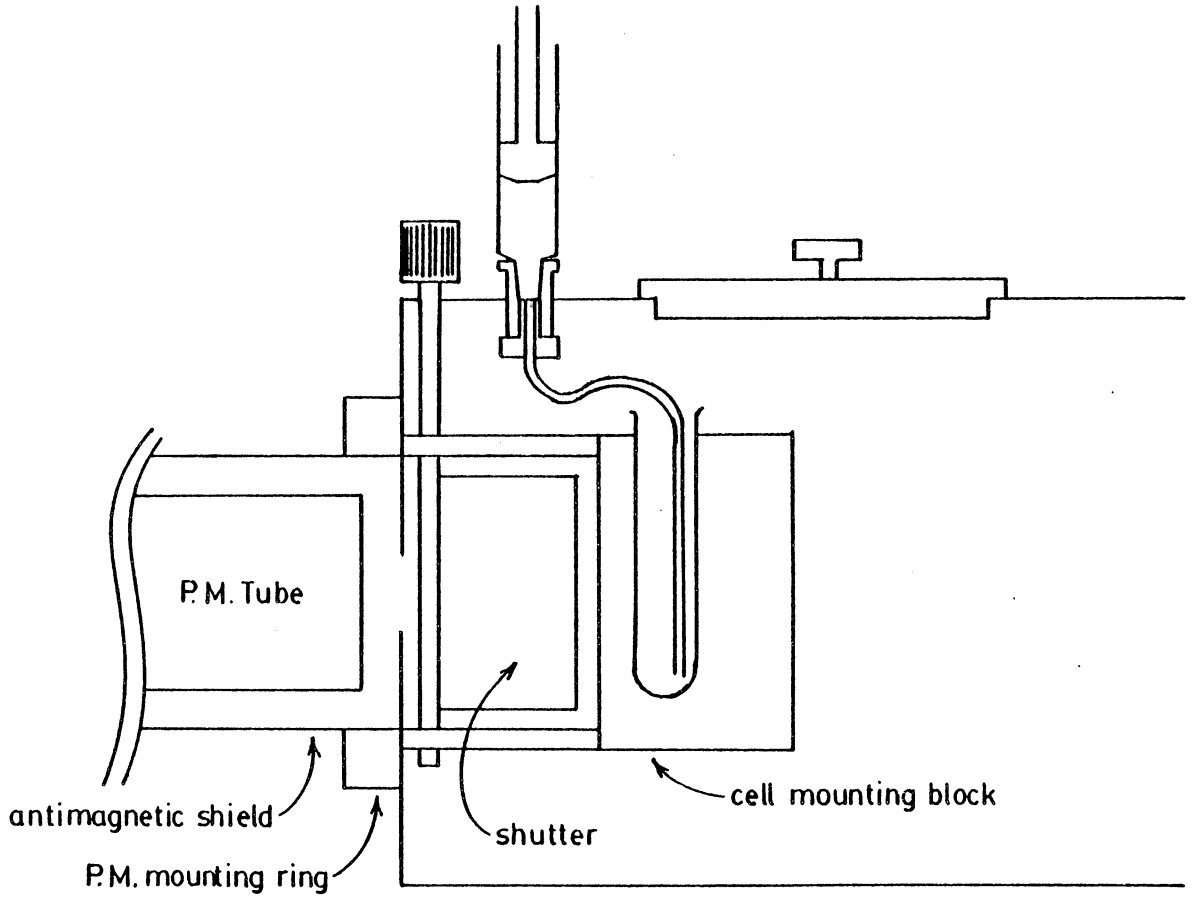

Figure 1. Diagram of manual luminometer.

lower reproducibility, which was due to the manual injection technique, it did provide flexible adjustment of reaction conditions.

Automated Luminometer

The following sections describe the luminometer that was built for quantitation of the chemiluminescence produced by the reaction under study. Figure 2 shows an overall schematic diagram of the luminometer and the associated interfaces between it and the computer. Each one of the major components in this system will be described in detail.

Cell Design

The cell, as shown in figure 3, was fabricated in glass with a 1 cm cross section and a volume of approximately 1.75 ml. The three flat surfaces not directly in front of the photomultiplier were mirrored on the outside to help reflect as much light as possible toward the detector.

Three openings to the cell were provided by 1/4 in. O.D., 1 mm I.D. glass tubing. The two top tubes were for the inlet of liquids and the venting of air

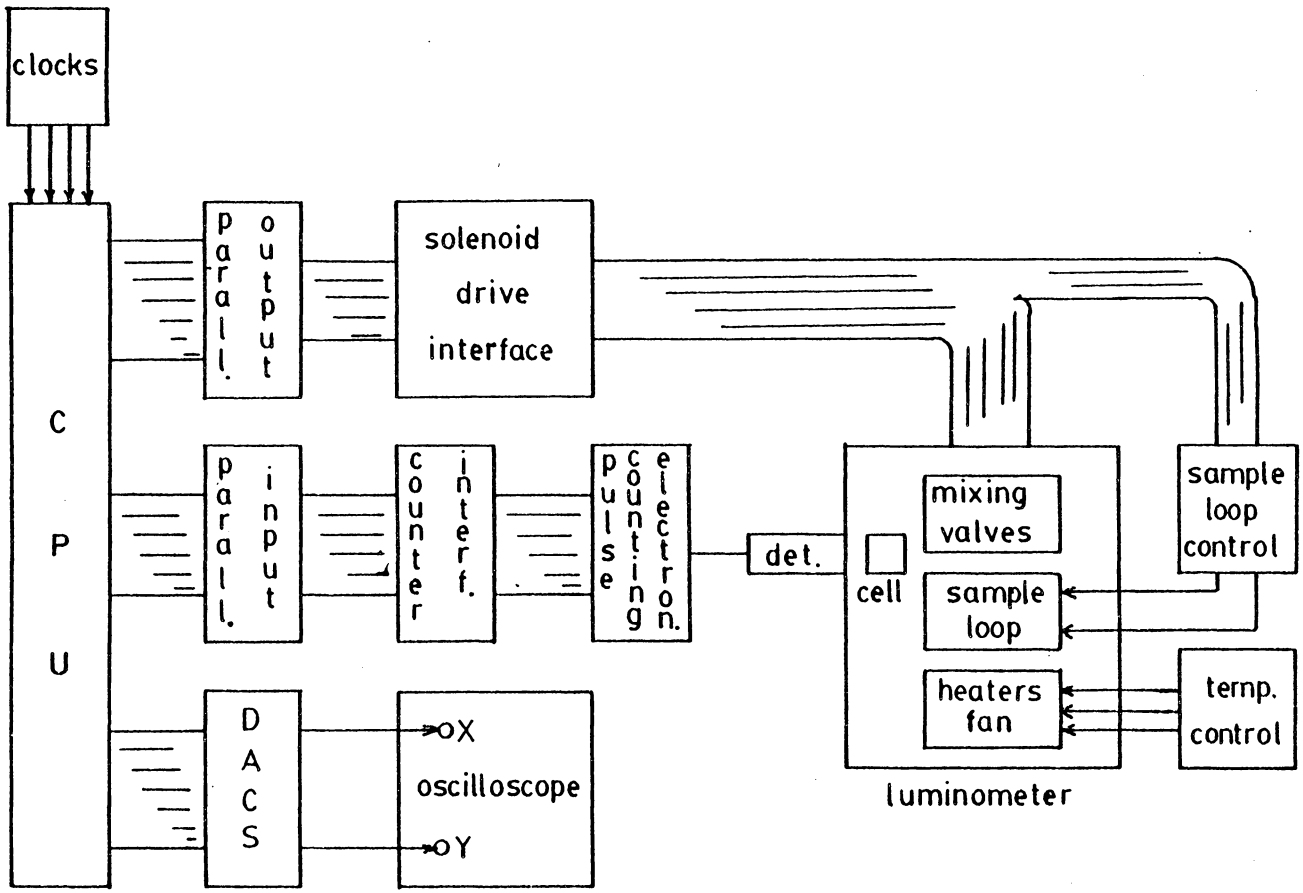

Figure 2. Diagram of automated luminometer.

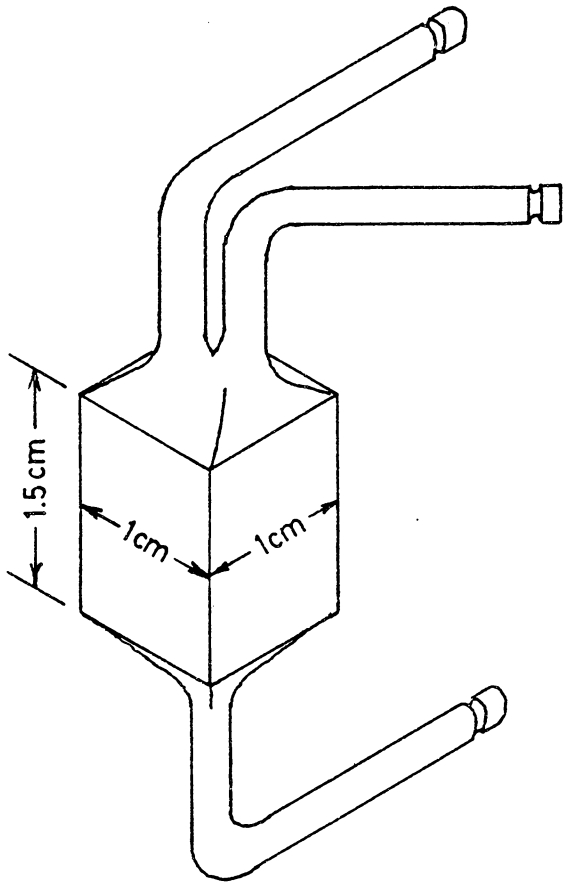

Figure 3. Luminometer cell design.

respectively. The vent also doubled as a gas inlet for purging the cell of the spent reagents. These upper ports were positioned at an angle of about 30 degrees to each other to provide space for the valves which were connected to them. The lower tube acted as a drain for the release of the spent reaction components after a run. Connections to the tubes were made with Cheminert 1/4-28 Teflon-to-glass adaptors. An aluminum block, which was machined to accept the square body of the cell, was used to fasten it to the inside wall of the luminometer directly in front of the photomultiplier.

Sample Injection System

The sample and reagent streams were mixed just outside of the cell at a Teflon mixing tee as shown in figure 4. The volumes of liquids injected into the cell were controlled by two General Valve Series 9 solenoid valves. The entire injection system upstream of these two valves was pressurized to a pressure of 80 psig from an external nitrogen tank. Therefore, to inject a sample the two series 9 solenoid valves were opened simultaneously and the pressure behind the liquids would force them into the mixing tee where mixing occurred before entering the cell. The series 9 solenoid valves were selected because

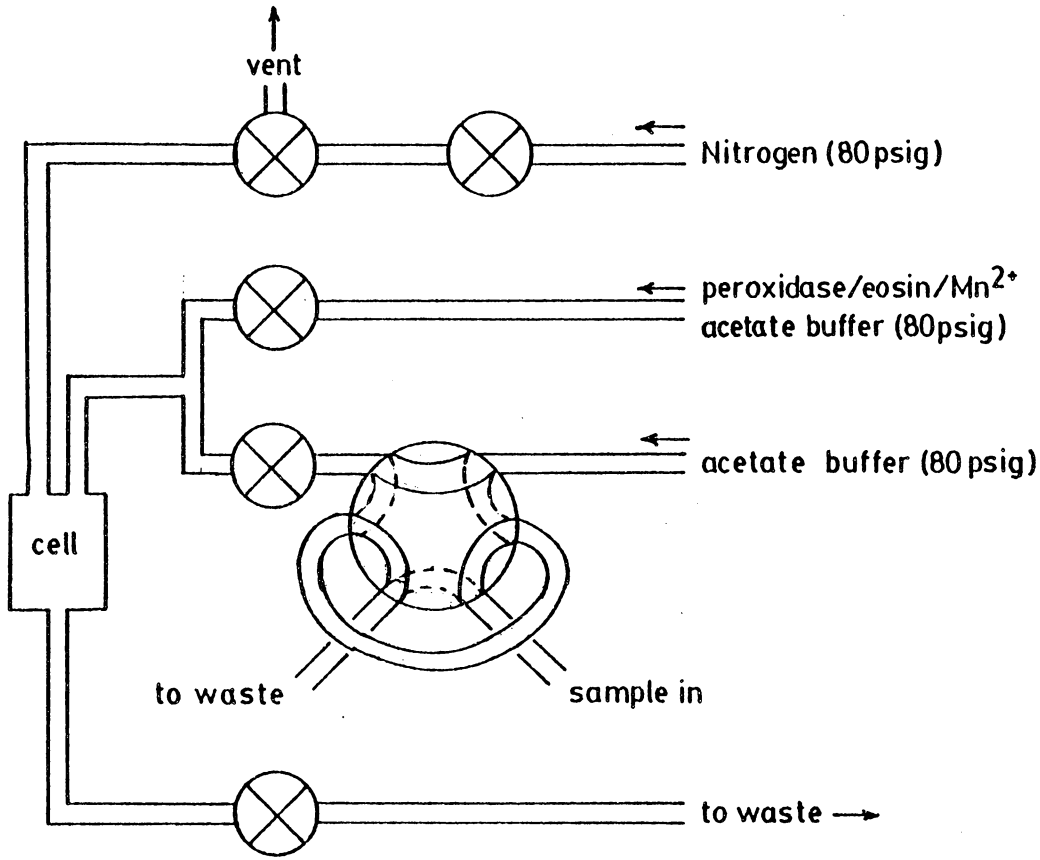

Figure 4. Schematic diagram of automated injection system.

they have an open/close cycle time of 2 ms which gives very good control over the volume of liquid injected.

The volume of sample actually injected into the cell was controlled by a pnuematically actuated chromatographic sample loop with a 0.5 mL volume. The contents of this loop was flushed into the cell with a stream of acetate buffer. The volume of the reagent stream injected was simply controlled by the amount of time for which its injection valve was left open. This was calibrated to give 0.5 mL of reagent per run.

Calibration of Injection System

To verify that the series 9 solenoid valves gave an injection volume that was linear with respect to open-time, and to develop the associated calibration curves, various volumes of liquid were injected into a glass weighing bottle and weighed on an analytical balance. The mass of the injected liquid, which is proportional to the injected volume, was then plotted against the valve open-time to give the calibration curves in figure 5. The regression line for the reagent curve is: $Y = 1.06\times10^{-2} + 1.34\times10^{-3}X$; $r^2 = 0.9999$; $S_{yx} = 3.75\times10^{-3}$. For the sample curve the regression line is: $Y = 1.72\times10^{-3} + 1.26\times10^{-3}X$; $r^2 = 0.9994$; $S_{yx} = 9.2\times10^{-3}$.

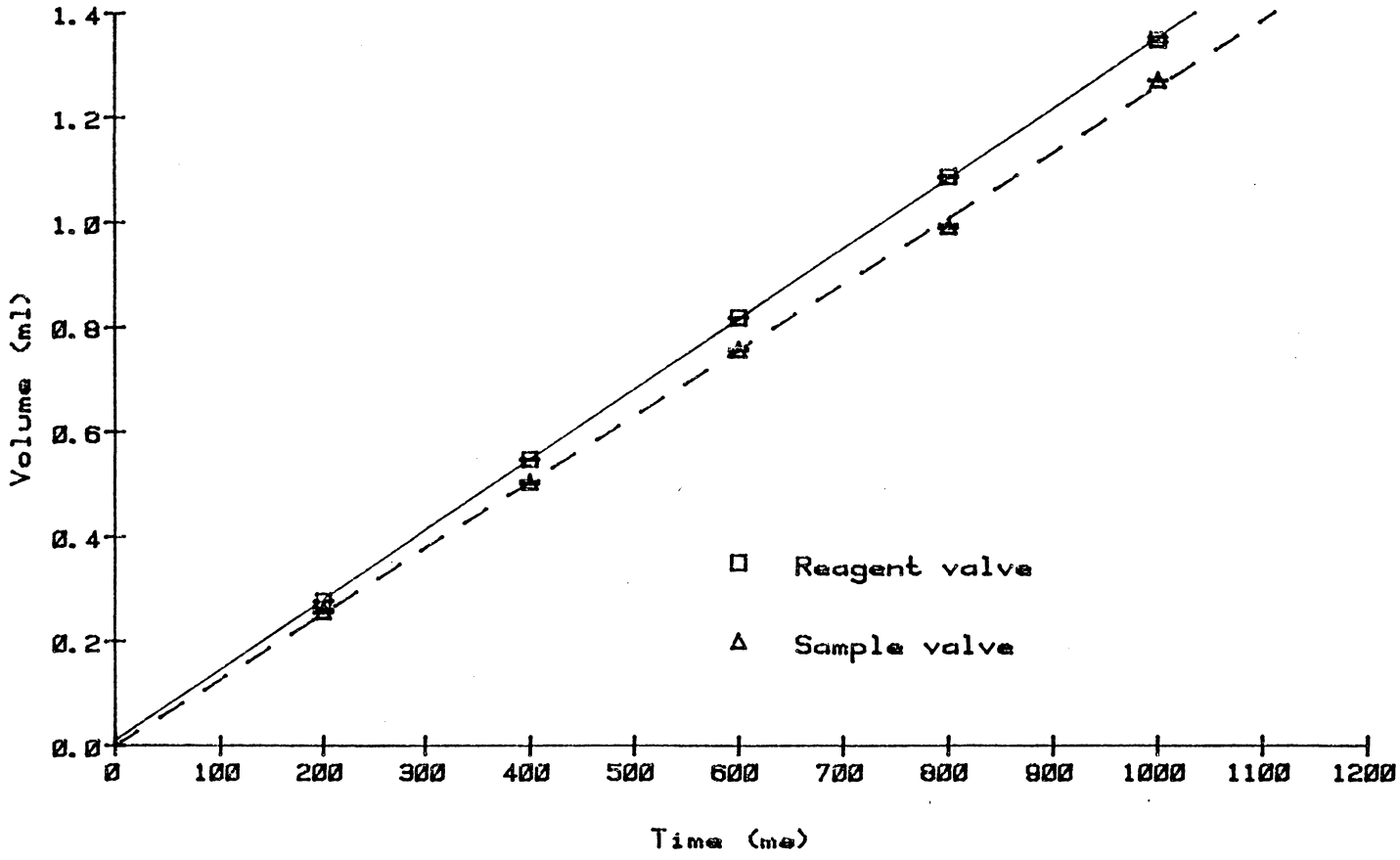

Figure 5. Calibration curves for injection valves.

The differences in the slopes of the two calibration curves is due to the fact that the cross sectional areas of the tubing differ. The sample stream must flow through the ports in the chromatographic sample valve which have a 0.8 mm inside diameter, whereas the reagent stream has 1 mm Teflon tubing as its smallest restriction.

To determine how long to open the sample injection valve, to insure that the complete sample was entering the cell, a green dye was loaded into the loop and the valve opened until no green color was visible in the tubing between the sample loop and the cell. This time was then used as the sample injection time in all subsequent runs.

Cell Rinsing System

Another series of valves were provided for the emptying and rinsing of the cell following a run. This operation was not nearly as time critical as the injection, so slower, less expensive series 3 solenoid valves from General Valve were employed.

A rinse sequence consisted of a number of discrete steps. Firstly, to empty the cell the drain valve was opened, the vent valve was switched into the flush position and the gas inlet valve was opened to pressurize the cell and force the liquid out. A separate gas inlet

valve was found to be necessary because the three way vent valve would not hold the 80 psig. while in the vent position. Secondly, the cell was rinsed with acetate buffer by switching the sample loop into the load position and opening the sample injection valve to fill the cell with buffer. This charge of buffer was then flushed out using the procedure described above. Finally, the last remaining liquid in the cell was blown out with nitrogen by opening the gas inlet valve again for several seconds. The drain valve was closed and the vent valve switched back into the vent position ready for the next injection.

Valve Control Interface

The control of the solenoid valves from the computer required its own interface, shown in figure 6, because the TTL outputs from the parallel port cannot supply the current needed to energize the solenoids. At 12 VDC the Series 3 valves draw about 200 mA and the Series 9 valves draw about 750 mA. The TTL circuitry associated with each output bit of the parallel port is only capable of supplying 1.6 mA.

Each of the Series 3 valves was driven with a 75152 core memory driver. This 8 pin chip takes a TTL input and is capable of switching up to 300 mA with its transisitor

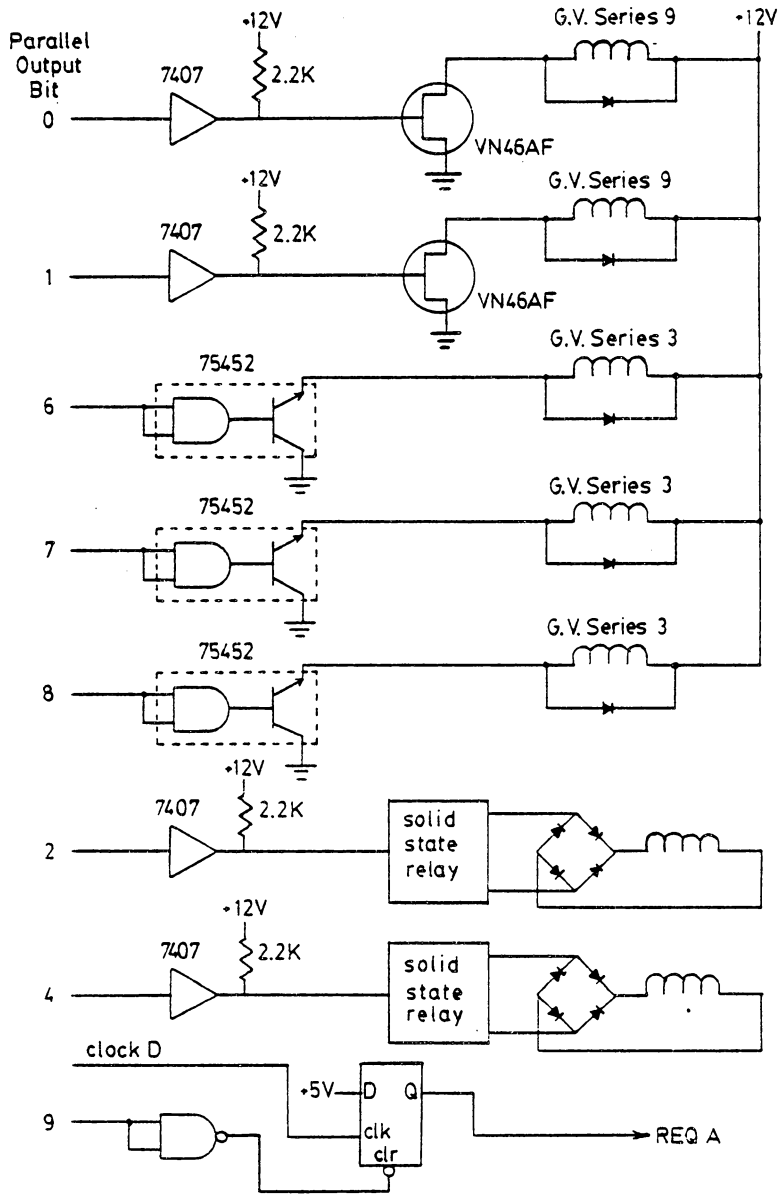

Figure 6. Schematic of solenoid valve interface.

output.

The Series 9 valves were switched with Silconix VN46 VMOS field effect transistors. Ideally, these FETs should allow the direct interfacing of TTL circuitry to high current devices drawing as much as 2A at 12 VDC. In this case, however, the power available from an individual output bit of the parallel port was not sufficient to saturate the gate of these devices, thus preventing them from switching enough current to open the Series 9 valves. This problem was cured by driving the gate of the FET with a 7407 open collector driver.

The nitrogen supply required to actuate the sample loop was also controlled by two output bits from the parallel port. The pneumatic pressure was actually switched by a pair of 110 VDC solenoid valves. The 100 VAC, which is rectified to 110 VDC, is switched by a pair of solid state relays. These solid state relays can be activated by the TTL signals from the parallel port. However, since they were located approximately three feet from the computer, it was decided to insert 7407 open collector drivers between the parallel port and the solid state relays.

Temperature Control

In kinetically controlled systems it is essential to maintain a constant temperature to ensure consistent reaction rates. Ambient temperature variations throughout the course of a year were sufficient to warrant the design and construction of a temperature control system for the luminometer. A temperature of 35^{o}C was chosen as the temperature to be maintained, as it was unlikely that indoor ambient temperatures would ever exceed this value. Since a single temperature was to be maintained throughout, it was not considered necessary to use computer control. A commercially available controller, RFL Industries (Boonton, NJ) model 72A with a model 27687-3 thermister, was installed. In addition to the controller a heating source and a circulating fan was necessary. To conserve space inside the luminometer, a commercial hair dryer was modified to provide both of these required components. As manufactured the hair dryer fan is wired in parallel with one of the heating elements which means that the heaters must be on to run the fan. Before it could be used the fan had to be separated from the heater circuit to allow the fan to be run continuously; the heating elements could then be switched

on and off, as necessary, by the temperature controller.

Figure 7 shows a schematic of the hair dryer circuit before modification. The motor is a 24 VDC type. The 24 VDC is achieved by using the three heating elements as a voltage divider and tapping off across the smallest element and feeding it to a bridge rectifier which in turn drives the motor. To provide separate fan control the input leads to the rectifier were clipped and connected to a separate AC supply through a step-down transformer.

Variable fan speeds were achieved by means of a HEXACON soldering iron controller. This is a silicon controlled rectifier based device which simply transmits varying fractions of the AC sine wave through to its load to control the amount of power delivered. To provide a safeguard against the possibility of turning the heaters on without the fan running, a small amount of the 12 VAC voltage from the step down transformer was tapped off and rectified to 5 VDC. This DC potential switched a solid state relay which in turn switched the main AC supply for the RFL controller. If the fan is not running, no voltage is available to close the solid state relay and thus no power is available to the heating elements.

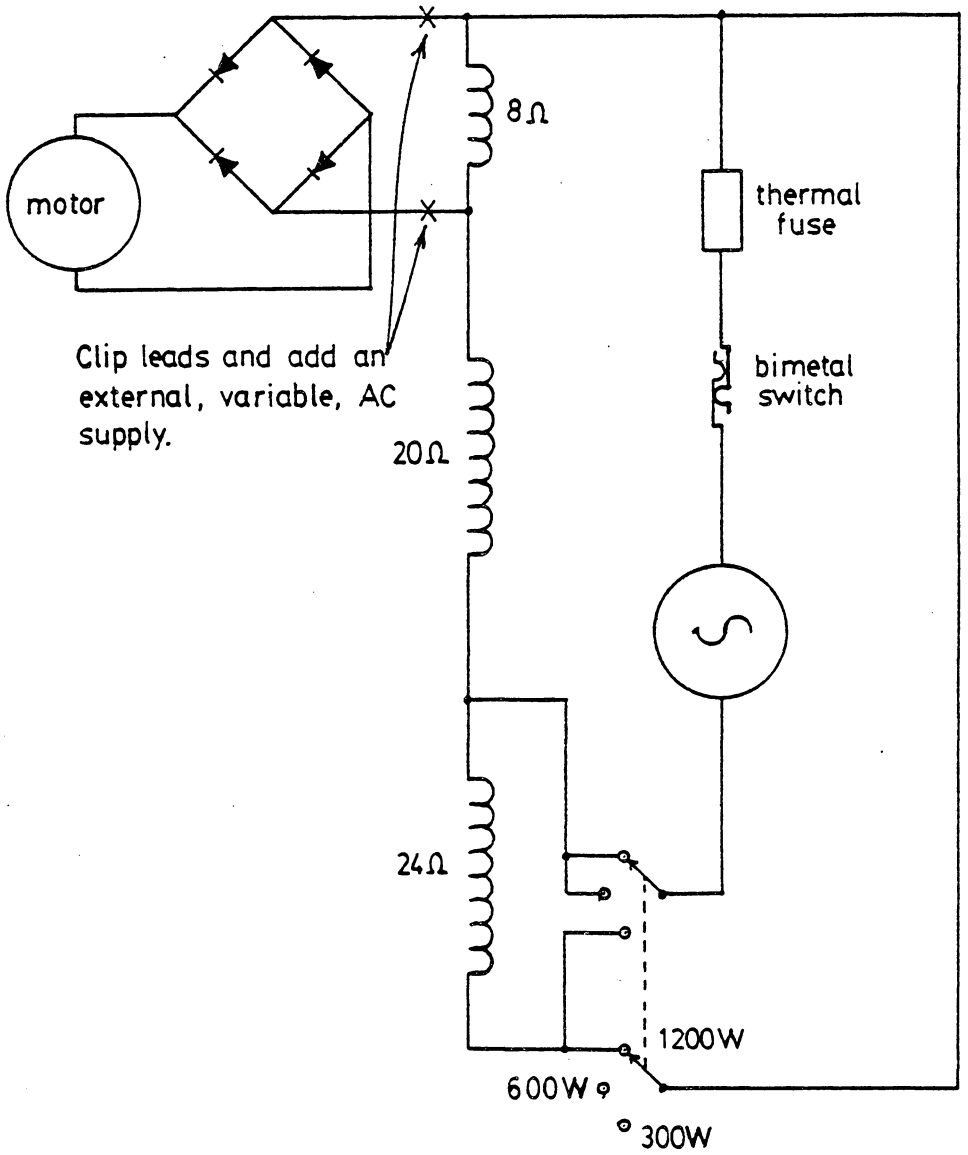

Figure 7. Schematic of hair dryer circuit.

Detector System

The detector used for the measurement of the luminescent intensity was an RCA (Lancaster,PA) 8575 photomultiplier housed in an Ortec (Oak Ridge, TN) model 265 photomultiplier base. The high voltage supply for this base was from as Ortec (Oak Ridge, TN) model 456 power supply which provided -2500 VDC to the cathode of the photomultiplier.

Current pulses at the photomultiplier anode, which result from the amplification of photoelectrons emitted from the photocathode, are converted into voltage pulses by an Ortec (Oak Ridge, TN) model 113 Preamplifier.

These discrete voltage pulses are then further shaped by an Ortec (Oak Ridge, TN) model 460 delay line amplifier. This amplifier narrows the incoming pulses by differentiating the input signal. A very sharp positive output spike is produced for the leading edge of the input pulse and a negative spike is produced for the trailing edge of the input pulse.

The amplitude of the output spikes coming from the delay line amplifier are then compared with an upper and a lower threshold voltage by an Ortec (Oak Ridge, TN) model 406A Single Channel Analyzer. The lower threshold voltage

is used to discriminate against small pulses which result from thermionic emision of electrons from one of the dynodes rather than the photocathode. These thermally produced electrons result in smaller output pulses at the anode because they undergo fewer stages of amplification than true photoelectrons from the photocathode. The upper threshold is used to discriminate against very large anode pulses which result, not from a photoelectric event at the photocathode, but from radioactive decay of trace radionuclides in the photocathode material. Therefore, to prevent being rejected, an anode pulse must be of sufficient amplitude to exceed the lower threshold voltage, but not be so intense as to also exceed the upper threshold value. For each input pulse which meets these requirements the single channel analyzer outputs a very narrow, TTL level square wave pulse which is then transmitted to a digitial counter.

The counter used in this detector is an Ortec (Oak Ridge, Tn) model 707 Buffer Scaler which is a decimal counter with a counting range from 0 to 999,999. It is a buffered counter, in that it contains a memory register to which the current count is transferred whenever it receives a reset signal. This permits a very small dead time, about 5 microseconds, between the initiation of a readout sequence and the resumption of counting. Once a

count has been buffered the computer can read the contents of the buffer register at its leisure while the counter continues to accumulate pulses over the next time frame. The number of pulses counted per unit time by the counter is therefore assumed proportional to the photon flux at the photocathode of the photomultiplier.

To ensure that this assumption is valid, it is important that the time frame between successive reads of the counter be precisely controlled. The time base used in this system was a crystal based, fixed period clock which was designed and built in house as a precise, general purpose clock source for automation applications. Figure 8 illustrates all of the components of the detector system.

Counter Interface

The Ortec (Oak Ridge, TN) 707 counter was not originally designed as a stand alone counter, but was intended by the manufacturer to be a member of a printout loop. This loop was a parallel bus which daisy chained a series of these devices together and allowed a single master controller to co-ordinate their activities. Due to its slow speed, the master controller, an Ortec (Oak Ridge, TN) model 432, did not easily lend itself to being

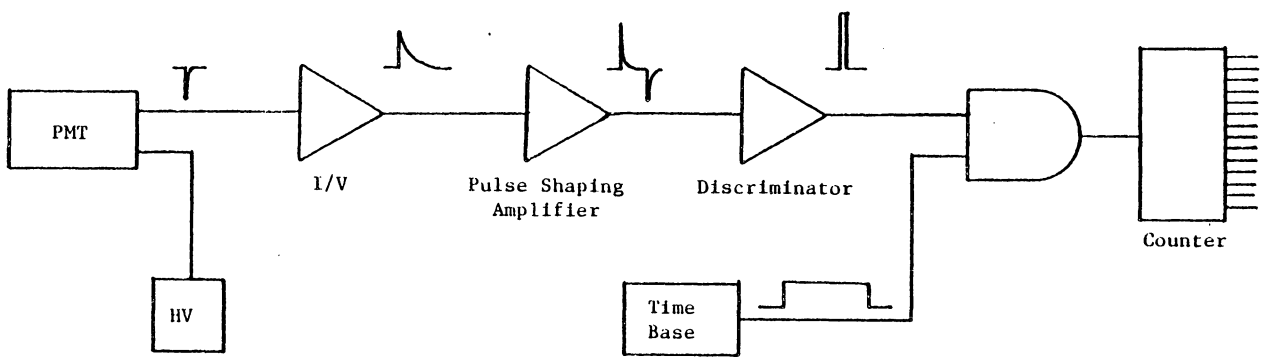

Figure 8. Schematic of pulse counting detector.

interfaced to a computer for rapid read out of the counter. Therefore, the printer loop and controller were replaced with a parallel interface which directly linked the counter and the computer's parallel port. This interface had to emulate those signals which were normally sent by the controller to the counter and had to be able to receive the accumulated count transmitted back by the counter.

Figure 9 shows a schematic diagram of the complete interface. All connections to the counter were made through the "Printer Loop In" connector on the rear panel and all counting was done in the "Buffer In" mode.

A read out sequence was initiated by pulling the System Preset line to a logic zero. This was originally meant to be a global signal sent to all counters on the loop to cause counting to be inhibited while each counter transferred its count to its own particular buffer register. Each counter would then reset to zero and resume counting.

Approximately 10 microseconds after System Preset goes low the Print line would be brought low. In the original loop system this was a signal to an individual counter to indicate that it was its turn to read out its contents.

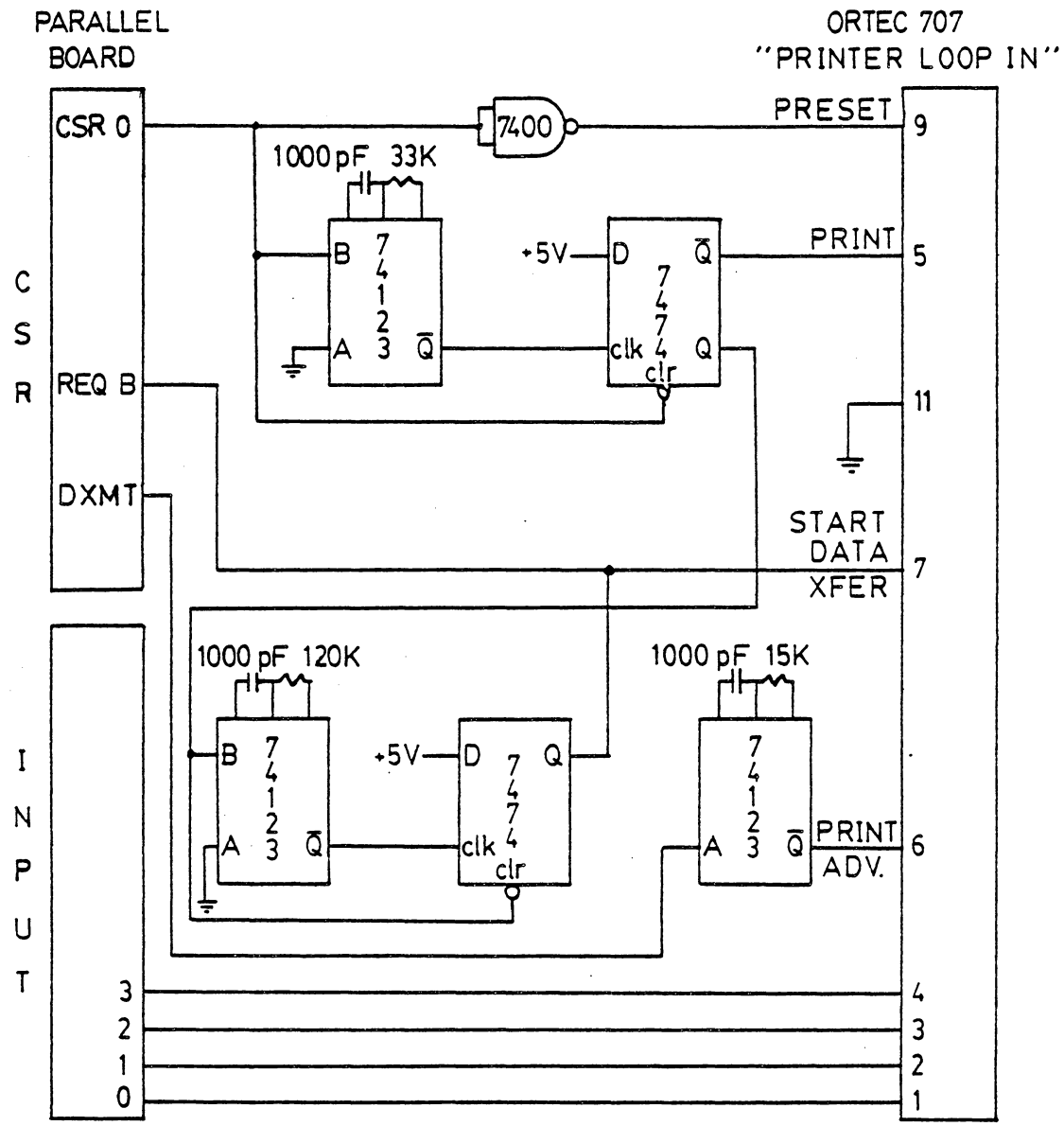

Figure 9. Schematic of digital counter interface.

The individual digits of the count are strobed out to the data lines serially as four bit, parallel, binary coded decimal numbers. The most significant digit of the count is gated onto the data lines when the Start Data Transfer line is asserted high, approximately 45 microseconds after Print goes low. This signal, like Print remains asserted until the completion of the read out sequence.

As each digit is read in through the parallel port the resulting DXMT pulse is stretched to a width of 5 microseconds, inverted and fed into the Print Advance input on the counter. Each time a Print Advance pulse is received the next digit in sequence is strobed onto the data lines. This process continues until all six digits have been read, at which time the Preset signal is released. The release of the Preset line causes the Print and Start Data Transfer signals to also be released, thus terminating the read out sequence.

Software

The Software used for the real time control of the luminometer and for the data acquisition made use of the multitasking capabilities of the polyFORTH (FORTH Inc., Hermosa Beach, CA) operating system. While all of the

software could have been incorporated into a single program it was decided, for the sake of ease of programming and maintainability, to break each one of the distinguishable jobs up into separate programs or tasks which would run concurrently.

Data Acquisition Task

The data acquisition task has two major functions. Firstly, the reading of counts from the pulse counting system at precise intervals and secondly the control of the valve actuation task. The less time critical portions are handled by a high level FORTH definition ACQUIRE, defined in block 309, which is the main definition used by the operator. ACQUIRE begins by turning on the pulse counting clock and counter, waits for counts and stores them in a data array as they arrive. After 60 counts have been received it instructs the valve control task to inject the sample and then continues to receive counts at the prescribed rate. When all of the data for a particular run has been collected, ACQUIRE disables the pulse counting system and instructs the valve control task to rinse the cell in readiness for the next run.

In a multiprogramming environment such as polyFORTH, the only way to to insure that the software reacts

immediately to an external event is to have that event cause a processor interrupt and have all time critical processing done by the interrupt service routine. The crystal based, fixed period clock, used for the pulse counting interval, interrupts the processor at a frequency of 10 hertz. Since the required data acquisition frequency is 5 hertz, data is only taken on every other interrupt.

Immediately upon entry to the interrupt service routine for this clock, defined in blocks 303 to 307, the software initiates a read out sequence by setting CSR0. The service routine then waits for the counter interface to respond with a Start Data Transfer signal and then begins to read in the sequential digits of the count. These binary coded decimal digits are assembled into a single 32 bit binary integer on the parameter stack before being passed back to the data acquisition task.

Since this value is to be passed back to the high level definition ACQUIRE, some care must be taken to insure that it is placed on ACQUIRE's parameter stack. When an asynchronous interrupt occurs in this type of operating system it is not possible to predict which task will be interrupted. Therefore, the interrupt service routine has to locate its calling task and then locate the parameter stack of that task before depositing the value

read from the counter. This particular operation is carried out by the code in lines 10 to 14 of block 303.

Valve Control Task

Throughout the operation of the luminometer all of the volumes of liquids injected are controlled by the amount of time the valves are open. The open time of the valves is controlled by software. Again to insure reproducible injection volumes this software has to be synchronized to a precise clock source. In one instance, the mixing of the sample stream with the reagent stream, two valves have to be open simultaneously but for different lengths of time. Therefore, two fixed period clocks are used by the valve control software. These two clocks are run at a relatively high frequency, 1000 Hz, to allow higher resolution of the volumes injected.

The valve control task consists of two time critical interrupt service routines, defined in blocks 313 and 314, which actually control the opening and closing of the valves. A number of less time critical high level definitions tell these routines which valves to open and for how long. A more detailed description of these high level definitions can be found in Appendix A.

Oscilloscope Display Task

A real time display of the raw data, as it is being acquired, is provided by a third task, defined in block 308. Being the least time critical, this task is not controlled by one of the fixed period clocks, but by the 60 Hz day clock.

The oscilloscope is operated in XY mode with one of the system's DACs connected to the vertical amplifier and the other DAC connected to the horizontal amplifier. After every third tick of the day clock the display task scans a single copy of the whole data array out to the vertical DAC while a constant voltage ramp is simultaneously scanned out to the horizontal DAC. This has the effect of producing a constantly updating XY display of the data set as it is being acquired.

Since the DACs only have a resolution of 2048 in the positive direction the display will begin to wrap around as the peaks exceed this limit. To help alleviate this problem the definition 1SCAN scales the data as it is being scanned out to the vertical DAC. After scaling the display will not wrap around unless a peak exceeds a value of 32,767.

Peak Processing

The total area of the luminescence peak represents the total light output which should be directly proportional to the concentration of the analyte of interest. However, as can be seen from figure 10, the luminescence peaks tail very badly. The trailing edge's very gradual approach to the baseline, combined with the inherent noise of the system, rendered the peak picking software quite unreliable in its ability to pick a consistent end of peak. As a result, the integrated peak areas were quite unreliable.

It became apparent, however, that the peak heights were giving a value proportional to analyte concentration that was reproducible. As previously described, 60 baseline data values were taken before the the sample and reagent streams were mixed. These 60 values were then averaged to give a mean baseline which was subsequently subtracted from the maximum value in the data set to yield the peak height. The background was sampled just prior to an injection to allow the maximum possible time for the baseline to have stabilize following the previous injection. The code to calculate the peak heights is listed in block 325.

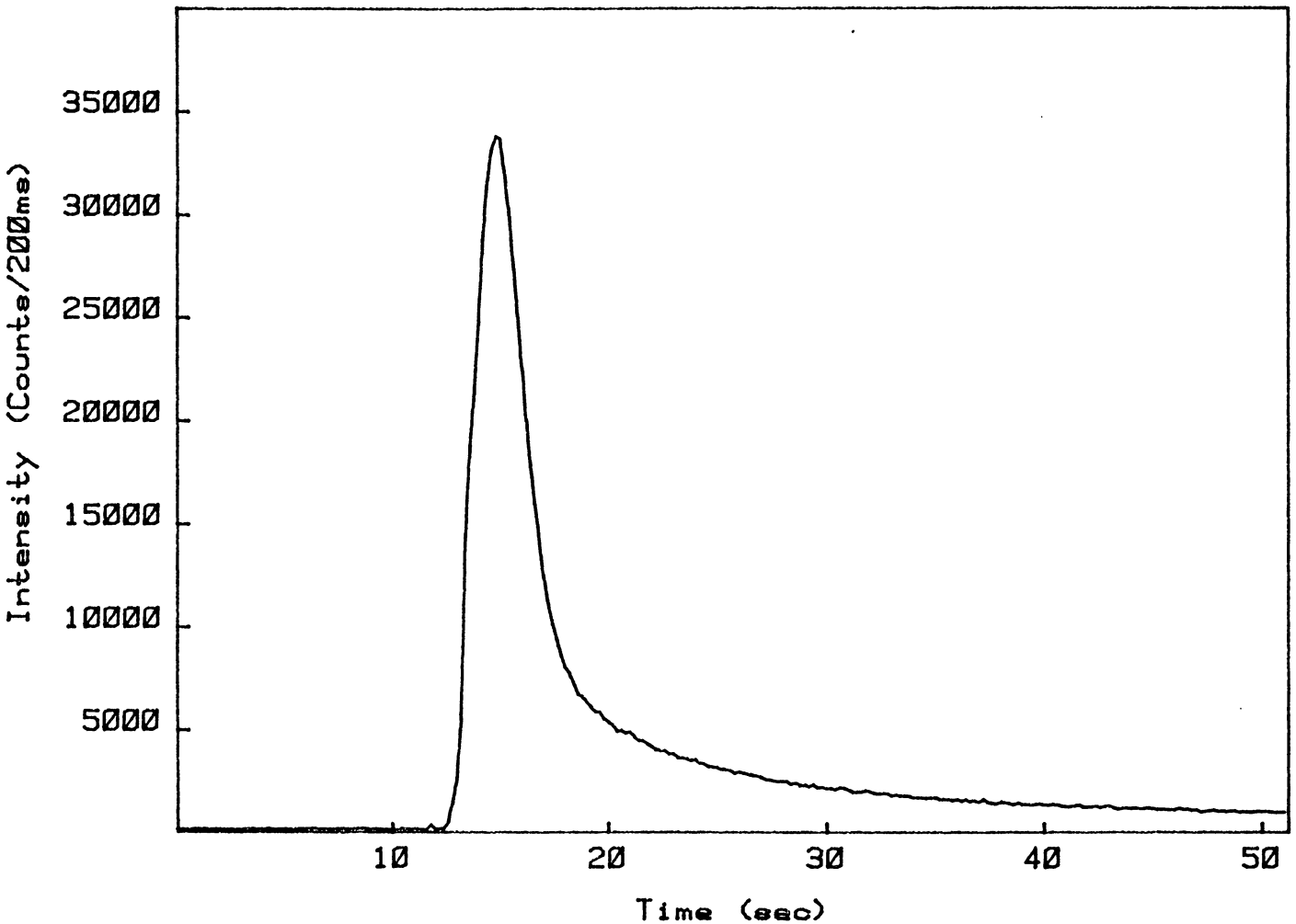

Figure 10. Typical chemiluminescence peak profile.

EXPERIMENTAL

The goal of this section is to determine if variations in the reaction conditions will provide an enhancement in the analytical signal. As can be seen from figure 20 (page 70) the chemiluminescent system under study does yield a linear relationship between the observed light output and the concentration of NADH being oxidized. When this particular reaction was reported by Cilento et. al. (6), no mention was made of analytical applicability or ideal reaction conditions. Therefore, it has been necessary to investigate each of the major reaction parameters with respect to their effects on analytical performance. The following describes the experiments performed in order to determine these effects.

Reagents

All biochemicals used in this study were from Sigma Chemical Co., P.O. Box 14508, St. Louis MO 63178. Horse radish peroxidase type VI was used throughout. Type VI peroxidase was selected due to its high RZ number, which is the ratio of the extinction coefficient at 403 nm to that at 278 nm. This number is often used as a qualitative indicator of the activity of a particular enzyme preparation. Zinner has reported that the type VI

peroxidase was much more effective, for this chemiluminescent reaction, than the less pure forms of peroxidase available from Sigma (22). The other enzymes used, such as alcohol dehydrogenase, glucose-6-phosphate dehydrogenase and formate dehydrogenase, were all from Sigma and had the highest available activities. Both the oxidized and reduced forms of NAD were from Sigma as were the various enzyme substrates and the Tris acid and base for the Tris buffers.

Acetic acid, sodium acetate and manganese chloride were obtained from Fisher Scientific, 3315 Winton Rd., Raleigh, NC 27604, while the disodium eosin was from American Research Products Co., P.O. Box 21009, South Euclid, OH 44121. The eosin from American Research Products had a reported dye content of approximately 90 percent and was the most pure form found. This compound was the only one that was further purified.

Eosin purification

The disodium eosin was dissolved in 0.1M ammonium hydroxide to a concentration of approximately 10 g/L. To remove neutral components this solution was extracted several times with equal volumes of diethyl ether and the organic layer was discarded. The free eosin was then

reprecipitated, according to the method of Marshall et. al., to remove any inorganic salts. The product was finally dried under vacuum at 100°C for approximately 12 hours. The melting point of 295-297°C for this free acid compared favorably with the published range of 295-296°C (23).

Since eosin is usually prepared by the bromination of fluorescein, it is likely that there will be traces of fluorescein present along with di- and tribromofluorescein (24). To test for these lower brominated fluoresceins, thin layer chromatography was carried out on the free acid according to the method described by Marshall and Lewis (25).

After elution for 24 hours, only two bands appeared. The main band was that of eosin and the smaller one was tribromofluorescein. A semiquantitative estimate of the amount of tribromofluorescein present was obtained by cutting out the two spots and dissolving them in 1% NH_4OH and recording their UV/Visible spectra. Using the extinction coefficients published by Mashall, Bentley and Lewis for dilute ammoniacal solutions of brominated fluoresceins (38), it was calculated that the recrystallized free acid of eosin contained approximately 15 percent tribromofluorescein. Due to the very similar structures of tribromofluorescein and eosin

(tetrabromofluorescein), it was not considered necessary to purify the dye further. All subsequent experiments were carried out using this recrystallized eosin.

Effect of pH

Based on their previous work, Cilento et. al. used a pH 4.2 acetate buffer as their standard reaction medium (22). This particular pH is quite low compared to that used with most enzyme reactions. If this chemiluminescent reaction is to be coupled to other enzyme reactions, which reduce NAD^+ to NADH, it would be highly desirable to have the chemiluminescent reation run at a higher pH.

To determine the sensitivity of the chemiluminescent reaction to pH, a series of 0.28M buffers varying in pH from 4.2 to 7.4 were prepared. Acetate buffers were used for the pH 4.2 and 5.0 cases, glycine for the 6.0 case and a Tris buffer for pH 7.4. Phosphate buffers are often used in the pH 6.0 range. However, in this instance a phosphate buffer could not be employed because the manganese would precipitate out as manganese phosphate.

Eosin was added to each buffer solution to give a final dye concentration of 3.8×10^{-5}M and $MnCl_2$ was added to give a manganese concentration of 1×10^{-3}M. Horse radish peroxidase was also dissolved in the buffer

solutions to a concentration of 0.15 mg/mL. A 1.5 mL aliquot of this solution was pipetted into the luminometer cell and the reaction was started by injecting 0.5 mL of an aqueous 2.2×10^{-4}M NADH solution.

Figure 11 shows a plot of the luminescence peak height as a function of the pH of the buffer. As can be seen from the plot, the luminescence intensity appears to be sensitive to the pH used. It was noted, qualitatively, that when the enzyme was added to the dye/manganese solution there was a shift in the color of the solution from an orange towards a red. This effect seemed strongest for the pH 4.2 case and decreased as the pH of the buffers increased.

The UV/Visible spectra of the dye/manganese/enzyme at both pH 4.2 and 5.0 appear in figure 12. As can be seen from these two spectra, the intensity of the 518 nm eosin band has decreased by about 30% with a concomitant increase in the absorbance at 230 nm. This may be suggesting that there is an enzyme/dye complex being formed which is responsible for the catalysis of the light emitting reaction.

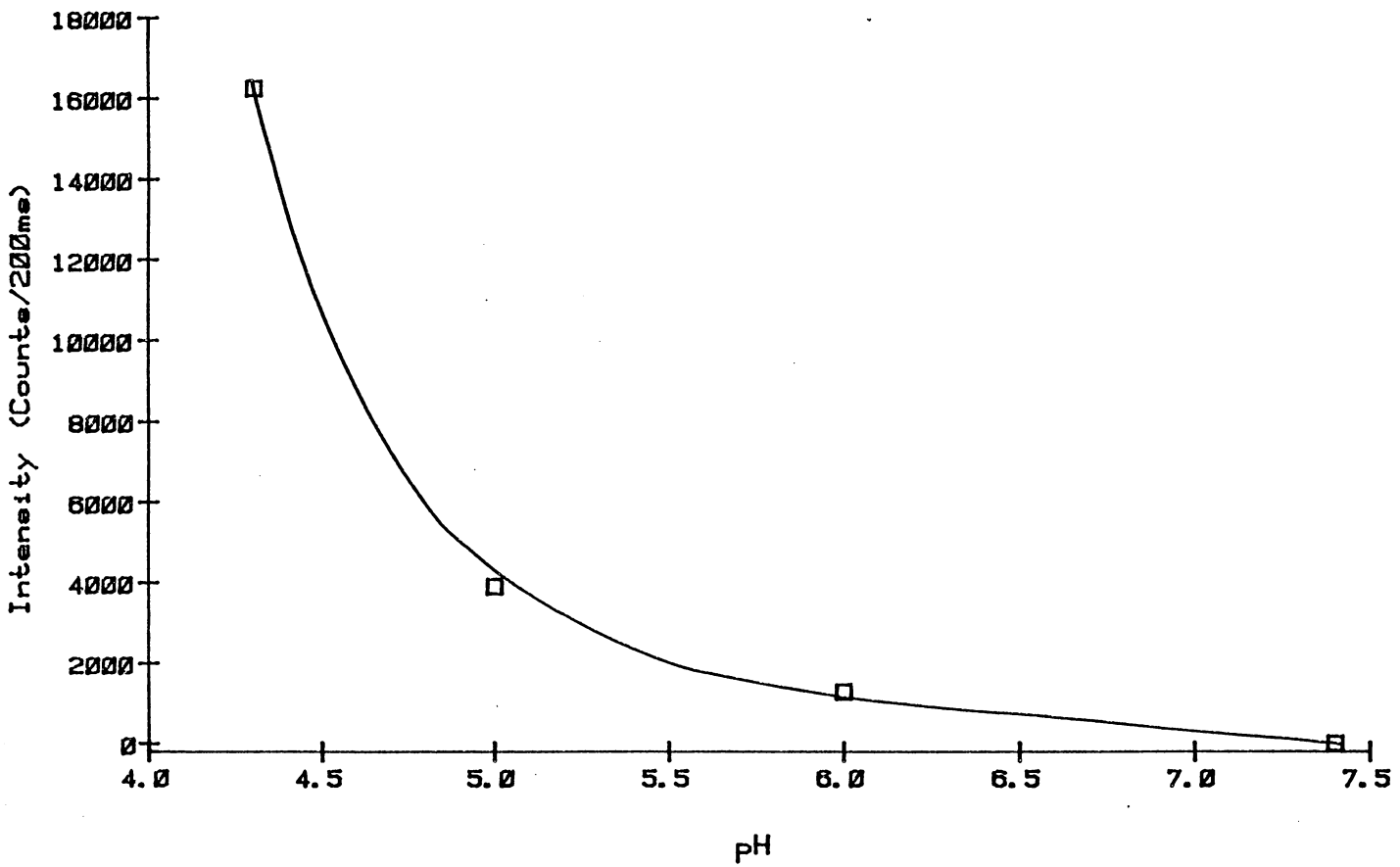

Figure 11. Light intensity as a function of buffer pH.

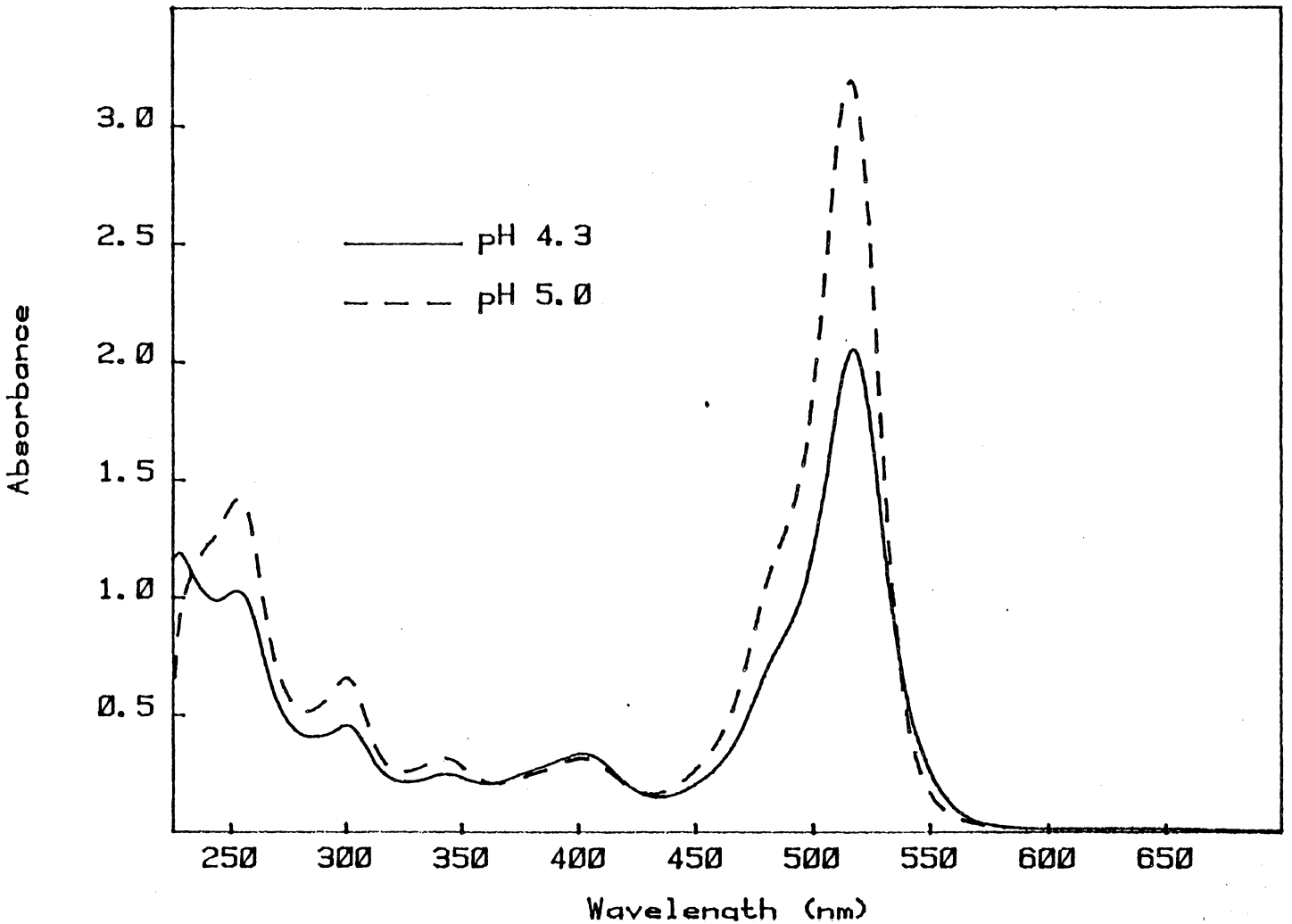

Figure 12. UV/Visible spectra of the peroxidase/eosin/Mn^{2+} solution at two different pHs.

Buffer Concentration

In addition to pH, the concentration of the buffer was checked for its effect on the light output. Even though there appears to be a requirement for a low pH, the high buffer concentration used by Cilento et. al. (6) may not be absolutely necessary. Again a lower buffer concentration would be desirable from the point of view of coupling this reaction to some other enzyme system.

Two pH 4.2 acetate buffers were prepared, one with a concentration of 0.28M and the other with a concentration of 0.028M. Eosin, $MnCl_2$ and peroxidase were added to these two buffers to produce solutions exactly as described above. Again, 1.5 mL of a buffer solution was added to the cell of the luminometer and the reaction initiated by injecting 0.5 mL of NADH. Figure 13 illustrates the rather dramatic effect that the decreased buffer concentration has on the light output. A number of other buffer concentrations, between 0.028M and 0.28M, were tried and gave a somewhat linear correlation btween buffer concentration and light output.

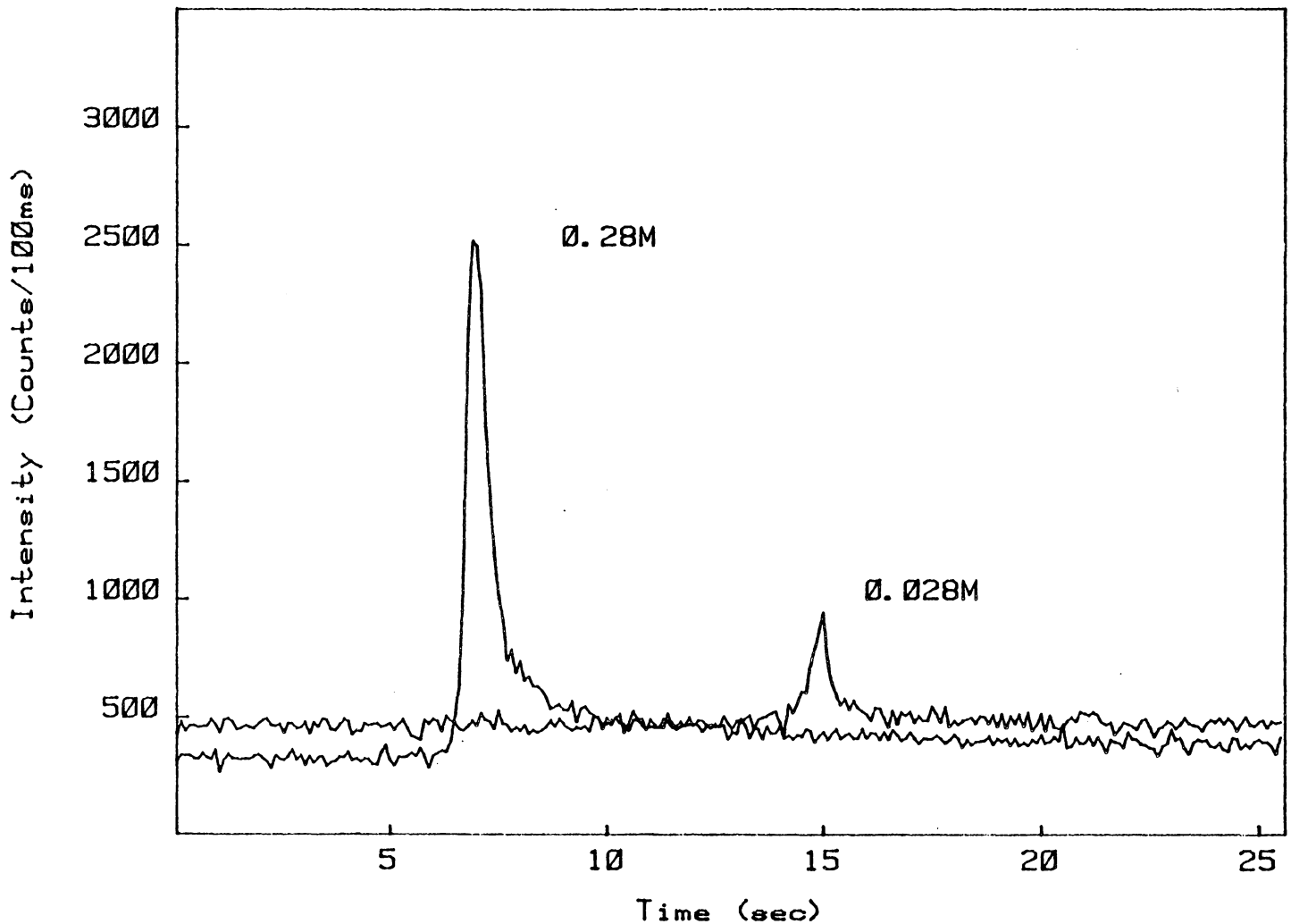

Figure 13. Luminescence output at two different buffer concentrations.

Manganese Concentration

The paper published by Cilento et. al. (6) describing this chemiluminescent reaction also included a description of a similar reaction which required a different Mn^{2+} concentration. Therefore, it was decided to investigate the effect of the Mn^{2+} concentration to see how sensitive the light emitting process was to manganese.

To investigate the effect of the manganese concentration on the light output, a $2x10^{-1}$M $MnCl_2$ solution was prepared in acetate buffer. Another stock solution containing $6.25x10^{-5}$M eosin and 0.15 mg/ml peroxidase was also prepared in acetate buffer. Five reaction mixtures were prepared containing 1 mL of the eosin/enzyme stock solution, varying amounts of the manganese stock solution and sufficient acetate buffer to bring the total volume up to 1.5 mL, as outlined in table 1. The chemiluminescent reaction was initiated by the injection of 0.5 mL of a deionized water solution containing $2.6x10^{-4}$M NADH.

Figure 14 shows a plot of the observed light output as a function of the manganese concentration. The drop-off in light intensity at low Mn^{2+} concentrations is consistent with earlier repetitions of this experiment.

Table 1

Composition of solutions for evaluation of light output as a function of Mn^{2+} concentration

Soln.	Vol. Eosin stock	Vol. Mn^{2+} stock	$[Mn^{2+}]$
1	2.0 ml	0.1 ml	9.92×10^{-5} M
2	2.0 ml	0.5 ml	4.96×10^{-4} M
3	2.0 ml	1.0 ml	9.92×10^{-4} M
4	2.0 ml	5.0 ml	4.96×10^{-3} M
5	2.0 ml	8.0 ml	7.93×10^{-3} M

eosin stock solution = 6.25×10^{-5} M

peroxidase concentration = 0.15 mg/ml

Mn^{2+} stock solution = 9.92×10^{-3} M

NADH concentration = 2.6×10^{-4} M

pH = 4.2

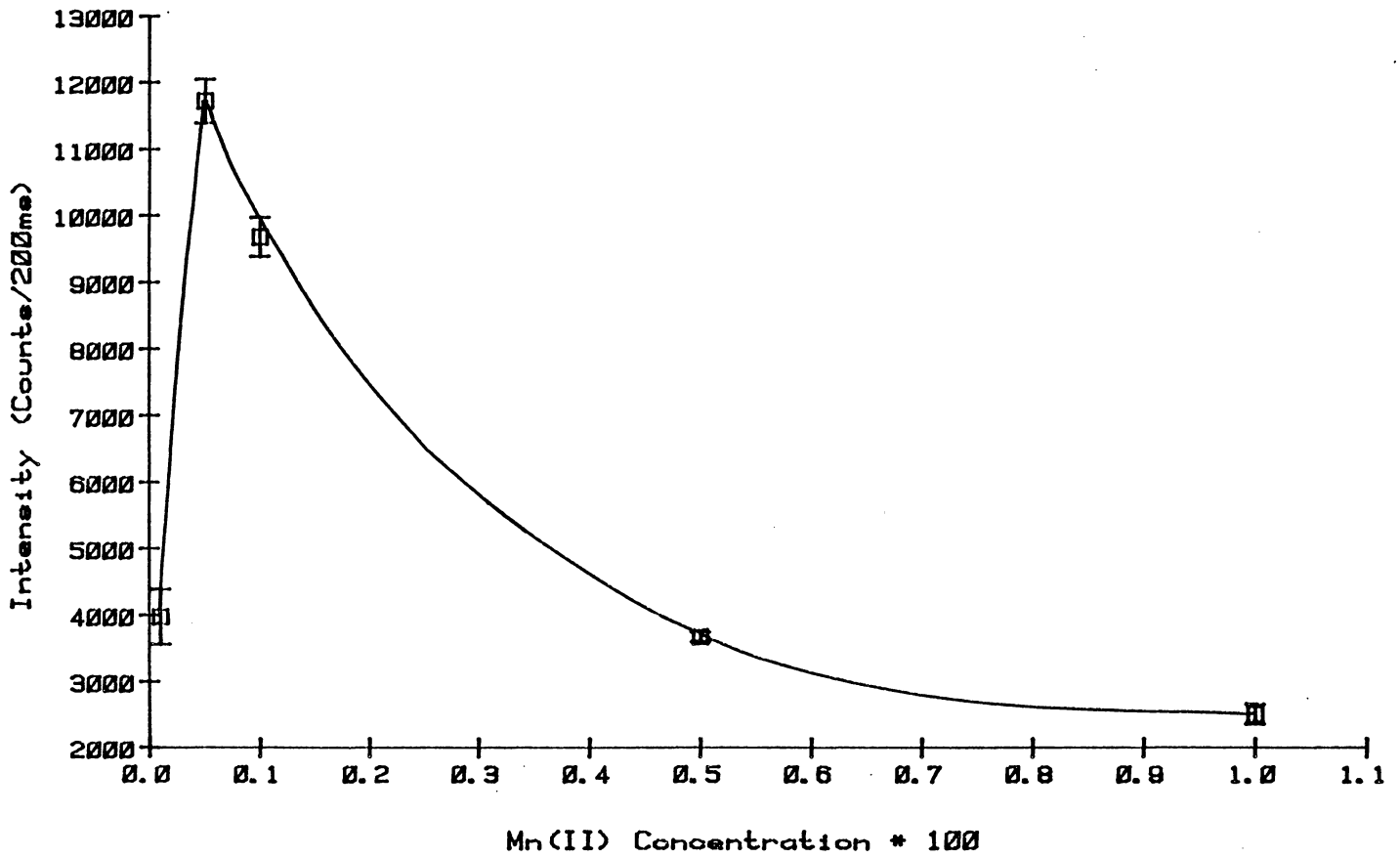

Figure 14. Light Intensity as a function of Mn^{2+} concentration.

As the Mn^{2+} concentration decreases the peak height decreases and also there is an increased lag time between injection and the onset of the peak.

Akazawa and Conn (18) had reported that at higher manganese concentrations, the rate of NADH oxidation decreased until oxidation became completely inhibited at around $1x10^{-2}M$. This may account for the drop in luminescence intensity at Mn^{2+} concentrations above $1x10^{-3}M$.

To investigate these possibilities a second experiment was undertaken to observe the rate of oxidation of NADH as a function of the Mn^{2+} concentration. NADH has a strong absorption band at 340 nm which is not present in the oxidized form. Therefore, the rate of oxidation can be followed by observing the rate of decease of this chromophore at different Mn^{2+} concentrations.

Five solutions were prepared containing 2 mL of $1.25x10^{-4}M$ eosin solution, varying volumes of a $1x10^{-2}M$ Mn^{2+} solution and sufficient acetate buffer to bring the total volume of each to 10 mL. 1 mL of each solution was pipetted into a 1 cm cuvette along with 0.5 mL of $1.63x10^{-4}M$ aqueous NADH and 0.5 mL of acetate buffer. The oxidation was initiated by the addition of 100 microliters of a 1 mg/mL peroxidase solution.

The rate of NADH oxidation, as measured by the rate of decrease of the 340 nm band, did increase with increasing manganese concentration over the entire concentration range used. In the cases where the NADH concentration was greater than $1x10^{-3}M$ the absorbance at 340 nm leveled off to a steady state value after the NADH had been oxidized and then began to increase again. It would seem unlikely that the oxidized NAD^+ was being reduced again so this increase in absorbance may result from some other reaction product which has some absorption at 340 nm.

Enzyme Concentration

Being the most expensive reagent in the reaction sequence, it was necessary to determine the minimum concentration of enzyme that would result in the maximum analytical signal. Therefore, an experiment was conducted to observe what effect peroxidase concentration has on the luminescent reaction.

Five solutions were prepared containing constant amounts of eosin and manganese but with varying amounts of peroxidase. Table 2 describes the various volumes of the stock solutions used. The eosin stock contained $1.25x10^{-4}M$ eosin and yielded a final dye concentration of

Table 2

Composition of solutions for evaluation of light output as a function of peroxidase concentration.

Soln.	Vol. Eosin	Vol. Mn^{2+}	Vol. HRP	final [HRP]
1	4.0 ml	1.0 ml	0.25 ml	0.009 mg/ml
2	4.0 ml	1.0 ml	0.5 ml	0.019 mg/ml
3	4.0 ml	1.0 ml	1.25 ml	0.047 mg/ml
4	4.0 ml	1.0 ml	2.5 ml	0.094 mg/ml
5	4.0 ml	1.0 ml	5.0 ml	0.188 mg/ml

eosin stock solution = 1.25×10^{-4} M

Mn^{2+} stock solution = 1.00×10^{-3} M

HRP stock solution = 0.75 mg/ml

NADH concentration = 4.7×10^{-4} M

pH = 4.2

$2.5x10^{-5}M$. Similarly, the final Mn^{2+} concentration for each one of the five solutions was $5x10^{-4}M$. The reaction was started by aliquoting 1.0 mL of a particular reaction mixture into the luminometer cell and injecting 0.5 mL of a $4.7x10^{-4}M$ aqueous NADH solution.

Figure 15 shows that, below 0.1 mg/mL, the peak height drops off fairly linearly with enzyme concentration. Associated with this decreasing peak heights is an increasing peak width and an increasing lag time between injection and the onset of the peak. Since all enzymes have finite rates at which they catalyze their characteristic reactions, it would not seem unreasonable that the peak heights should become shorter and broader at lower enzyme concentrations. This, however, does not explain the increased lag time between injection and the start of the peak. At lower enzyme concentrations, the rate of reaction [11] (figure 26) will be reduced. This will reduce the rate of reactions [13] and [14] which in turn will control the H_2O_2 need to sustain reaction [11]. A reduced rate of production of eosin radicals by reaction [11] will increase the time necessary to develop a photon flux which can be detected above the background.

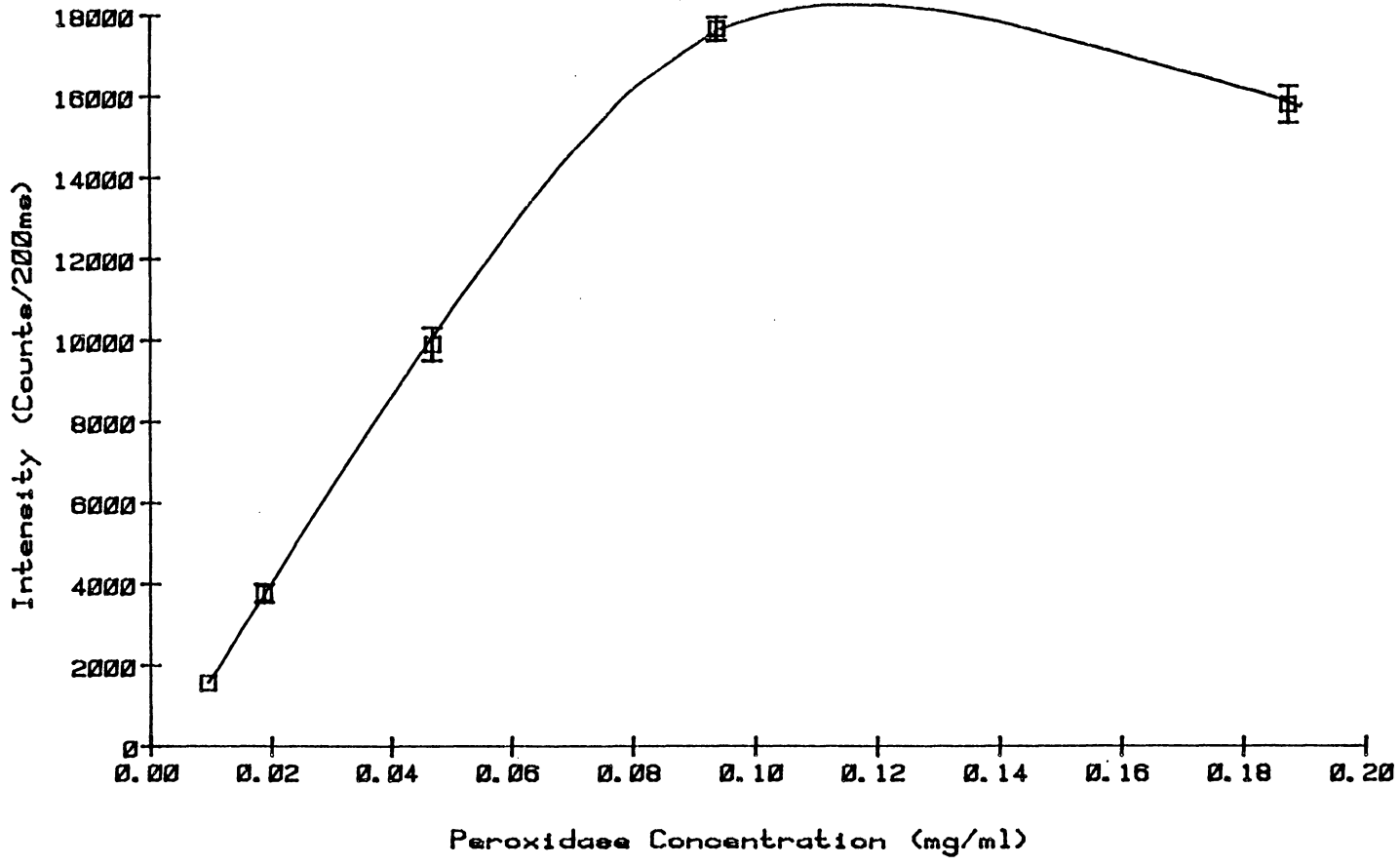

Figure 15. Light Intensity as a function of enzyme concentration.

Eosin Concentration

If the dye is being recycled as anticipated, it would be expected that the light output should be fairly independant of the eosin concentration. On the other hand if the dye is being consumed irreversibly by the reaction rather than being recycled, one might expect some sort of linear function between the eosin concentration and the light output.

To determine the sensitivity of the reaction to dye concentration, four reactions mixtures were prepared containing constant amounts of manganese and peroxidase and varying concentrations of eosin. Table 3 shows the compositions of the four solutions. The manganese stock had a concentration of 1.0×10^{-2}M and yielded a final Mn^{2+} concentration of 5.0×10^{-4}M. The peroxidase was diluted to a final concentration of 0.078 mg/mL and the eosin stock solution had a concentration of 1.11×10^{-4}M. A reaction was initiated by first pipetting 1.0 mL of a particular reaction mixture into the luminometer cell followed by 0.5 mL of acetate buffer and finally injecting 0.5 mL of a 1.03×10^{-4}M aqueous solution of NADH.

Figure 16 shows that the light intensity drops off with decreasing eosin concentration. This is not the type

Table 3

Composition of solutions for evaluation of light output as a function of eosin concentration.

Soln.	Vol. HRP	Vol. Mn^{2+}	Vol. Eosin	final [Eos]
1	1.0 ml	1.0 ml	1.0 ml	5.55×10^{-6} M
2	1.0 ml	1.0 ml	2.0 ml	1.11×10^{-5} M
3	1.0 ml	1.0 ml	5.0 ml	2.78×10^{-5} M
4	1.0 ml	1.0 ml	8.0 ml	4.44×10^{-5} M

eosin stock solution = 1.11×10^{-4} M

Mn^{2+} stock solution = 1.00×10^{-3} M

HRP stock solution = 1.56 mg/ml

NADH concentration = 1.03×10^{-4} M

pH = 4.2

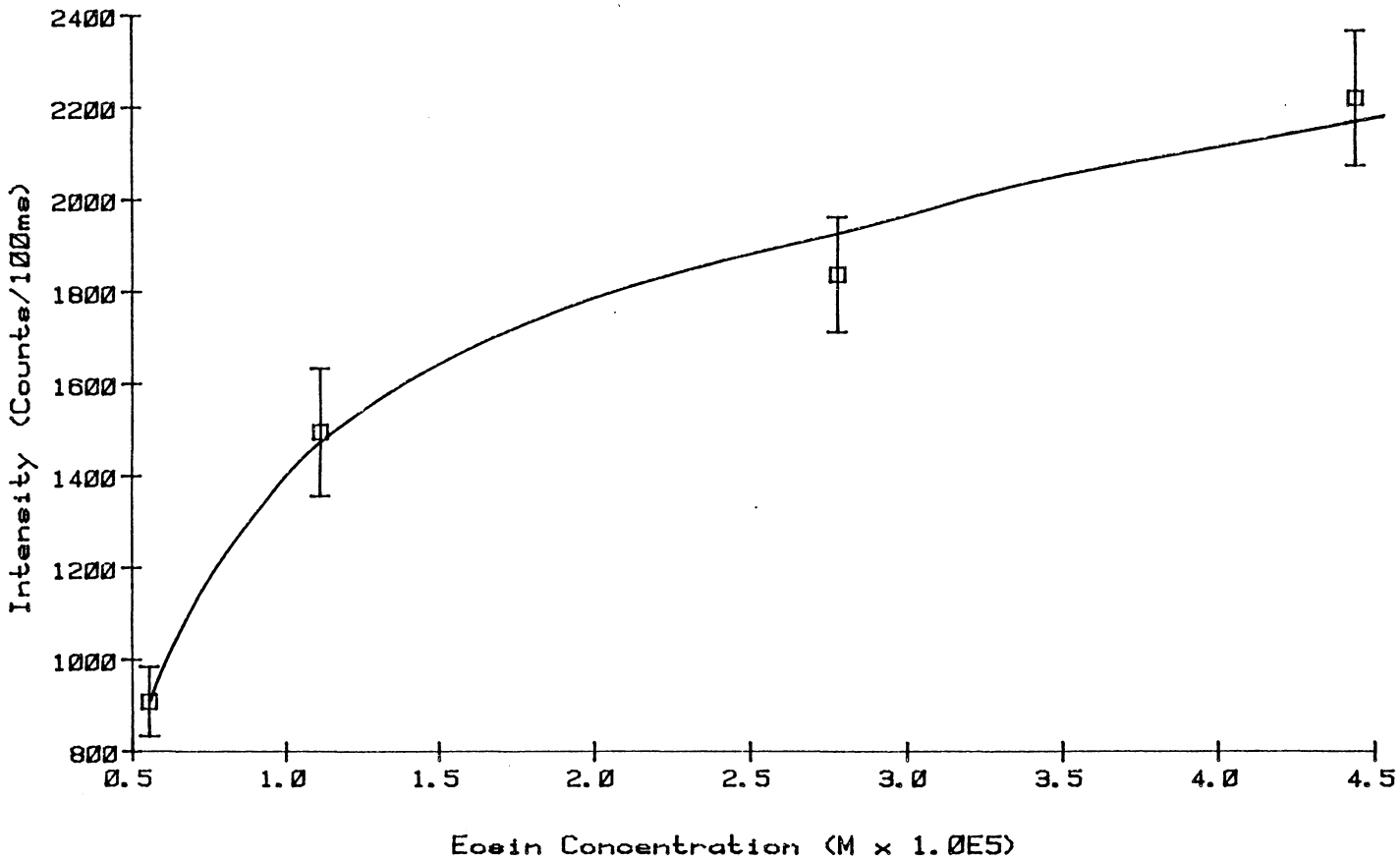

Figure 16. Light Intensity as a function of eosin concentration.

of response expected if the dye was indeed being recycled. Ideally the response should have been independent of the dye concentration. It was observed, however, that as the dye concentration was decreased the orange color of the dye was being bleached by some process associated with the chemiluminescent reaction. This bleaching could be measured as a decrease in the absorbance of the 518 nm band of eosin. At sufficiently low dye concentrations the spent reaction mixture would be rendered completely colorless.

It became apparent that the degree of bleaching was related loosely to the ratio of the dye and NADH concentrations. Figure 17 illustrates the observed relationship between the amount of dye lost and the amount of NADH oxidized. These data were obtained by observing the decrease in the 518 nm absorption band of eosin after the addition of various concentrations of NADH.

The lower part of the curve shows a linear trend which would be expected from a stoichiometric relationship between the eosin and the NADH. However, the reduced rate of bleaching at higher NADH concentrations was unexpected.

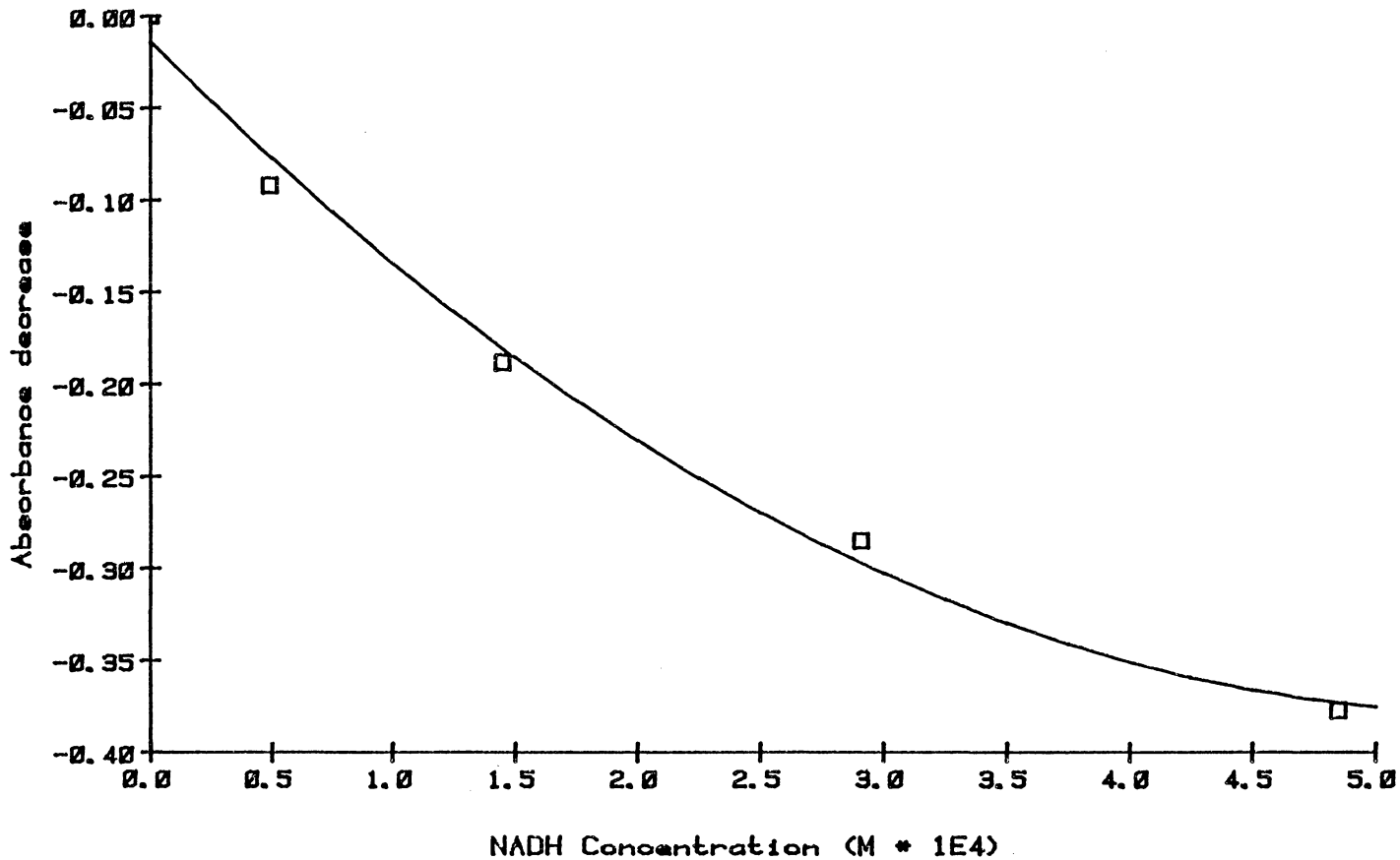

Figure 17. Decrease in the absorbance of the 518 nm band of eosin as a function of the NADH concentration.

Oxygen

The mechanism proposed for the oxidation of NADH by peroxidase (figure 26) incorporates molecular oxygen in a non-enzyme mediated chain reaction (20). Therefore, one might expect the photon emission to be influenced by the oxygen levels in the solutions. To observe this influence, the luminescence from an NADH sample was recorded in the usual manner. The normal dissolved oxygen level was then forced closer to its saturation point by bubbling oxygen through both the enzyme/dye/Mn^{2+} solution and the NADH solution, by means of a 1 mm Teflon tube, for approximately 30 minutes. After this 30 minute exposure to pure oxygen, the luminescence from the same NADH sample was recorded again. Figure 18 shows the luminescence spectra before and after exposure to oxygen.

Conversely, the equilibrium dissolved oxygen concentration can be lowered by bubbling nitrogen through the solutions and again one might expect this to reverse the trend observed with the added oxygen. Using the same procedure as described above, the luminescence from an NADH sample was recorded before the addition of nitrogen and again after exposure to nitrogen for 30 minutes. Figure 19 shows the result of this exposure to added

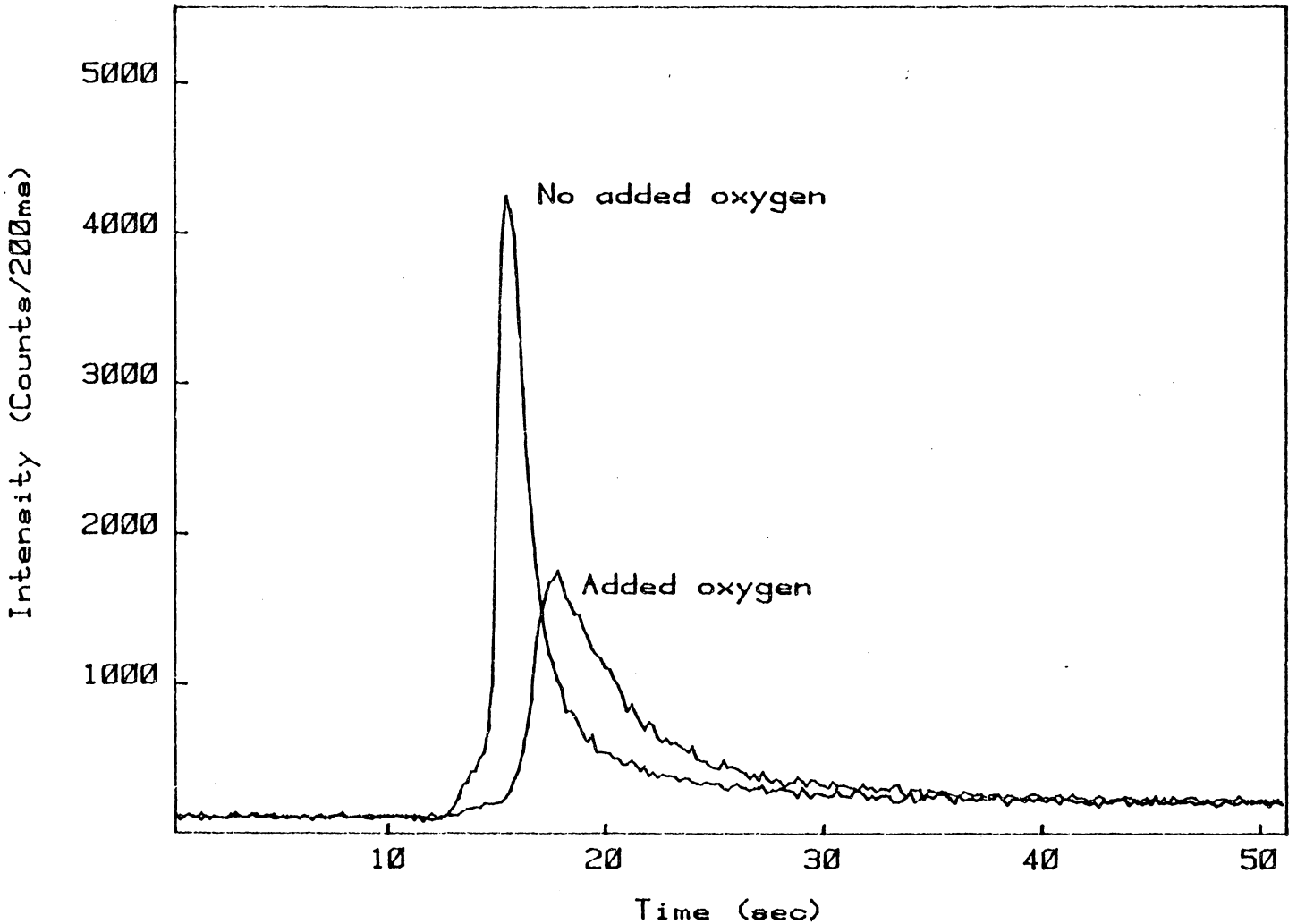

Figure 18. Luminescence output with and without added oxygen.

nitrogen.

An unexpected observation was that after about 15 minutes of bubbling with nitrogen, the red-orange color of the enzyme/dye complex disappeared leaving only the orange color of the dye itself. The red-orange color did not immediately return after rebubbling with oxygen. However, after this sealed flask had been allowed to stand over night the red-orange color became clearly evident again.

NADH Response

Because of its higher precision, the automated luminometer was used to record the system response to NADH concentration. From previous work with the manual luminometer, it appeared that a dynamic range of two orders of magnitude should be possible with a lower limit of detection in the 10^{-6}M range. With this range in mind, five calibration solutions were prepared by diluting various volumes of an aqueous NADH solution which had a concentration of 5.19×10^{-4}M. These five solutions had concentrations ranging from 5.19×10^{-6}M to 5.19×10^{-4}M. Table 4 describes the actual volumes of NADH stock used and the resulting concentrations of the calibration solutions.

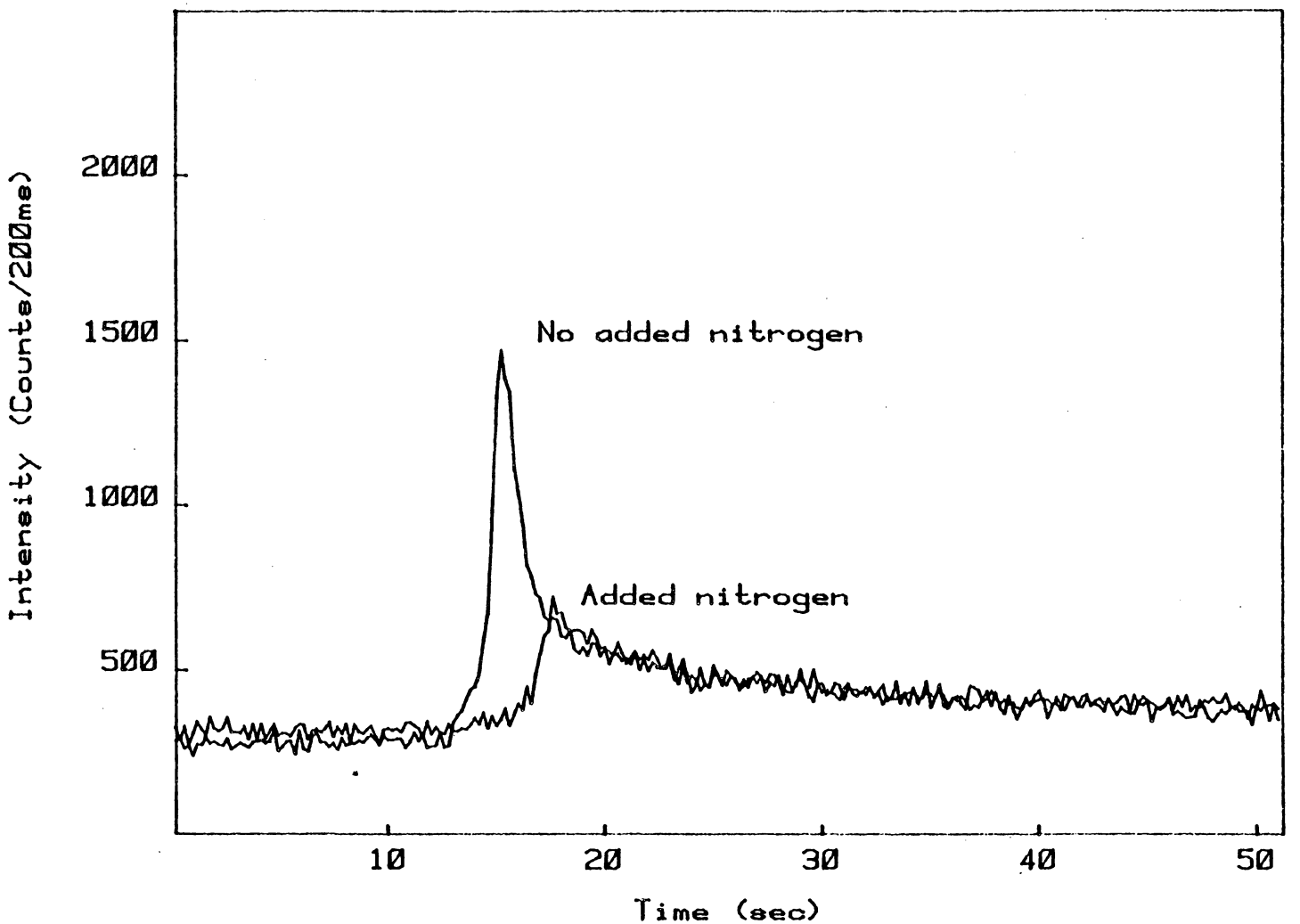

Figure 19. Luminescence output with and without added nitrogen.

Table 4

Composition of standard solutions used for NADH calibration curve.

Soln.	Vol. NADH stock	[NADH]
1	0.1 ml	5.19×10^{-6}M
2	1.0 ml	5.19×10^{-5}M
3	2.0 ml	1.04×10^{-4}M
4	6.0 ml	3.11×10^{-4}M
5	10.0 ml	5.19×10^{-4}M

NADH stock solution = 5.19×10^{-4}M

eosin concentration = 3×10^{-5}M

Mn^{2+} concentration = 1×10^{-3}M

peroxidase concentration = 0.2 mg/ml

pH = 4.2

The reagent reservoir was filled with a solution containing $3x10^{-5}M$ eosin, $1x10^{-3}M$ Mn^{2+} and 0.2 mg/mL peroxidase. The carrier reservoir was filled with 0.28M acetate buffer. A sample of each calibration solution was sucked into the sample loop, in turn, with a plastic syringe before the injection system was actuated.

Figure 20 shows the light intensity as a function of NADH concentration. Indeed a linear response was obtained over the desired two order of magnitude range between $5x10^{-6}M$ to $5x10^{-4}M$ NADH. The regression line is: $Y = -4.055x10^{2} + 8.957x10^{7}X$; $r^2 = 0.989$ and $S_{yx} = 1.903x10^{3}$. If one calculates the minimum detectable quantity, as that which produces a response three times the standard deviation of the background noise, a value of approximately $1x10^{-6}M$ is obtained.

Coupling to ADH

A number of enzymes, particularly the dehydrogenases, use NAD^+ as a cofactor. During the process of oxidizing their substrates, these enzymes also reduce NAD^+ to NADH. One of the most widely used dehydrogenase of this type is alcohol dehydrogenase (ADH). This enzyme oxidizes ethanol to acetaldehyde with a resulting reduction of NAD^+ to NADH.

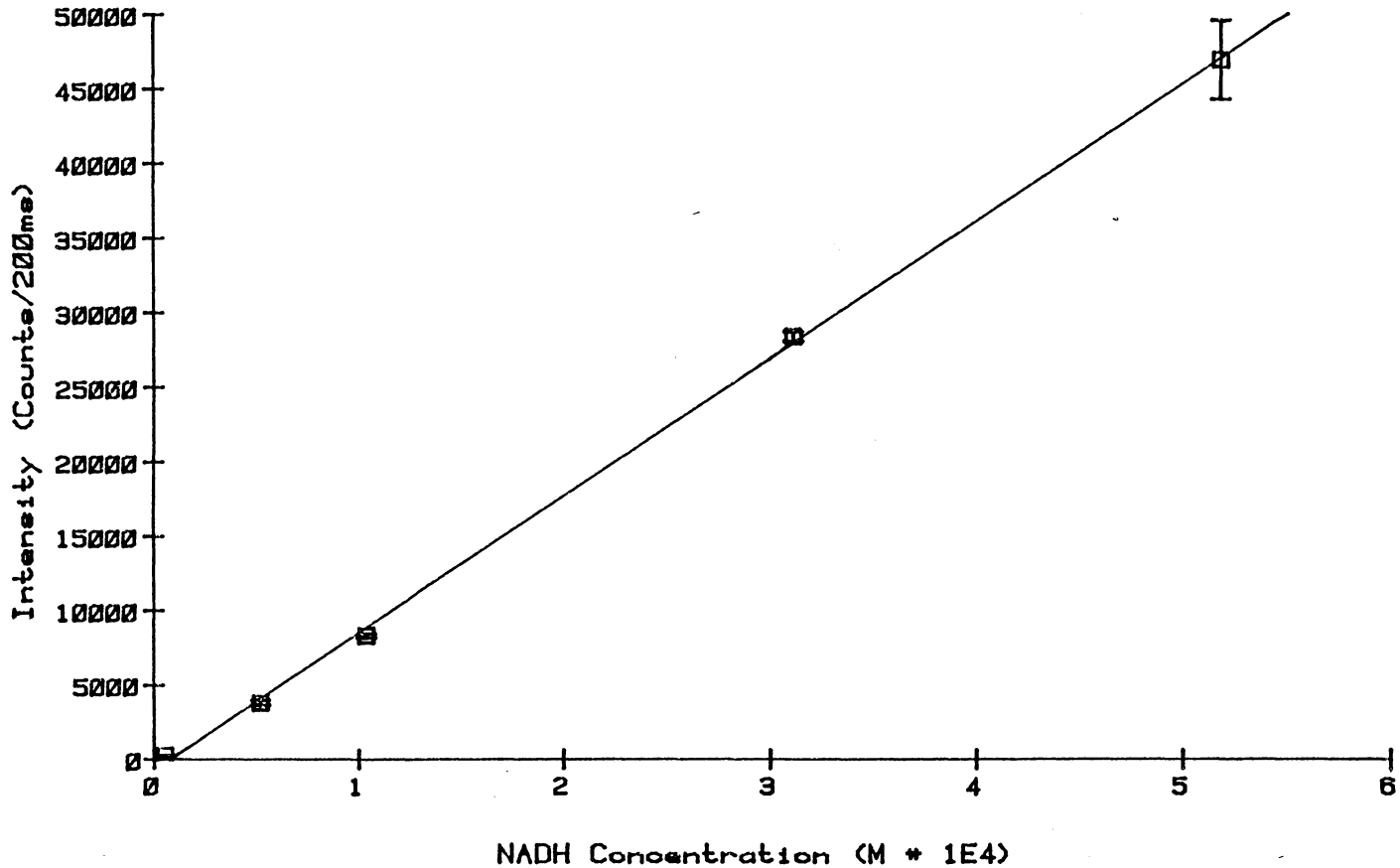

Figure 20. Light intensity as a function of NADH concentration.

$$\text{ethanol} + NAD^+ \overset{ADH}{\rightleftharpoons} \text{acetaldehyde} + NADH + H^+ \qquad [5]$$

In neutral solutions the equilibrium for the reaction lies far to the left. The equilibrium constant is as follows:

$$K = \frac{[\text{acetaldehyde}][NADH][H^+]}{[\text{ethanol}][NAD^+]} = 1.1 \times 10^{-11} \qquad [6]$$

it can be seen that there is only a small percentage of ethanol in the form of acetaldehyde. The two steps which are usually taken to force this reaction further to the right are to run it at a pH of 9 and to add a trapping agent for the acetaldehyde. Semicarbazide is a common trapping agent since it will form a semicarbazone with the acetaldehyde and prevent it from participating in the reverse reaction.

The requirement of a high pH for this reaction is an unfavorable one from the point of view of coupling to the chemiluminescent reaction. Mixing a pH 9 buffer with a pH 4.2 buffer would bring the overall pH up to a point where no chemiluminescence would be observed. Therefore, an experiment was conducted to see if the reaction would run at an appreciable rate with the aid of the semicarbazide but at a lower pH.

Three 0.01M Tris buffers were prepared with pH's of 7.6, 8.3 and 9.0. Each of these buffers were also made up to 0.01M semicarbazide, 1.4×10^{-4}M NAD^+ and 0.1 mg/mL alcohol dehydrogenase. A 3 mL aliquot of a particular buffer was pipetted into a UV/Visible cuvette and the reaction initiated by the addition of 100 microliters of 1.7×10^{-2}M ethanol. The rate of reduction of the NAD^+ was followed by watching the increase of the 340 nm band of NADH. As can can be seen from figure 21, the rate of NAD^+ reduction decreases with decreasing pH.

Some enzyme systems are sensitive to the nature of the buffer used. Therefore, the same experiment was carried out again, substituting a 0.01M glycine buffer for the Tris buffer. Again, as can be seen from figure 21, the rate of NAD^+ reduction decreases with decreasing pH and there seems to be little difference between the performance in glycine compared to that in Tris.

A pH 9 buffer could perhaps be tolerated if the concentration of that buffer was very low and 0.5 mL of such a solution was mixed with 1.5 mL of a very concentrated pH 4.2 buffer. To test the viability of using a very weak pH 9 buffer, four pH 9 Tris buffers were prepared with concentrations ranging from 0.01M to 0.5M. Each buffer contained 0.01M semicarbazide, 8.5×10^{-5}M NAD^+ and 0.05 mg/mL alcohol dehydrogenase. The reduction of

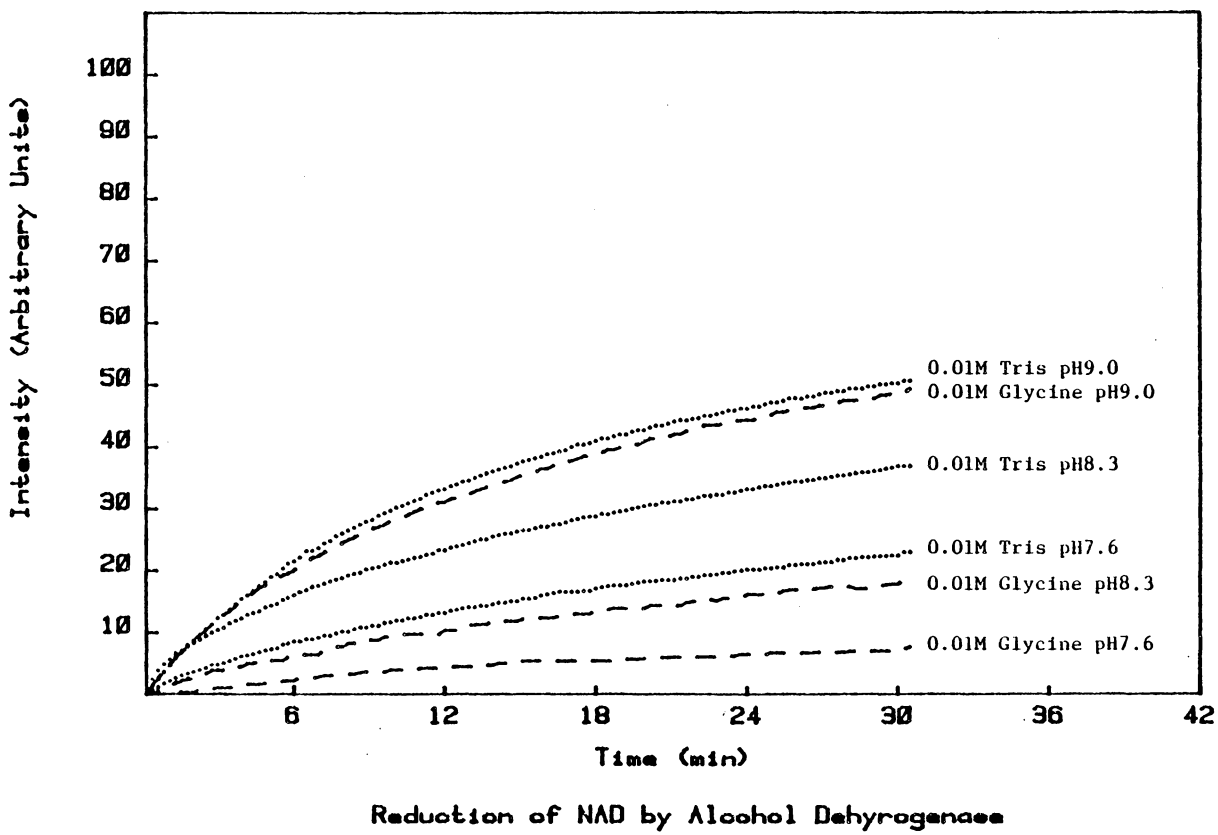

Figure 21. Rate of reduction of NAD^+ by alcohol dehydrogenase in two different buffers at various pHs.

the NAD^+ was initiated in the cuvette by the addition of 100 microliters of $1.7x10^{-2}$M ethanol. Figure 22 shows that the rate of NAD^+ reduction is also quite dependant upon the buffer concentration. This trend may be due, in part, to the fact that the reaction of the semicarbazide with the acetaldehyde is acid catalyzed (26). Based on alcohol dehydrogenase's dependance on pH and buffer concentration this enzyme would appear to be a poor candidate for the initial coupling to the chemiluminescent reaction.

Another common enzyme used for the determination of NAD^+ is lactate dehydrogenase. However, based upon the previous experiments with alcohol dehydrogenase, it too would seem an unlikely candidate, because its equilibrium constant is also very small:

$$K = \frac{[\text{pyruvate}][\text{NADH}][H^+]}{[\text{lactate}][NAD^+]} = 1x10^{-12} \qquad [7]$$

The same techniques are used to force this reaction to the right, namely the use of a high pH buffer and a trapping agent such as semicarbazide.

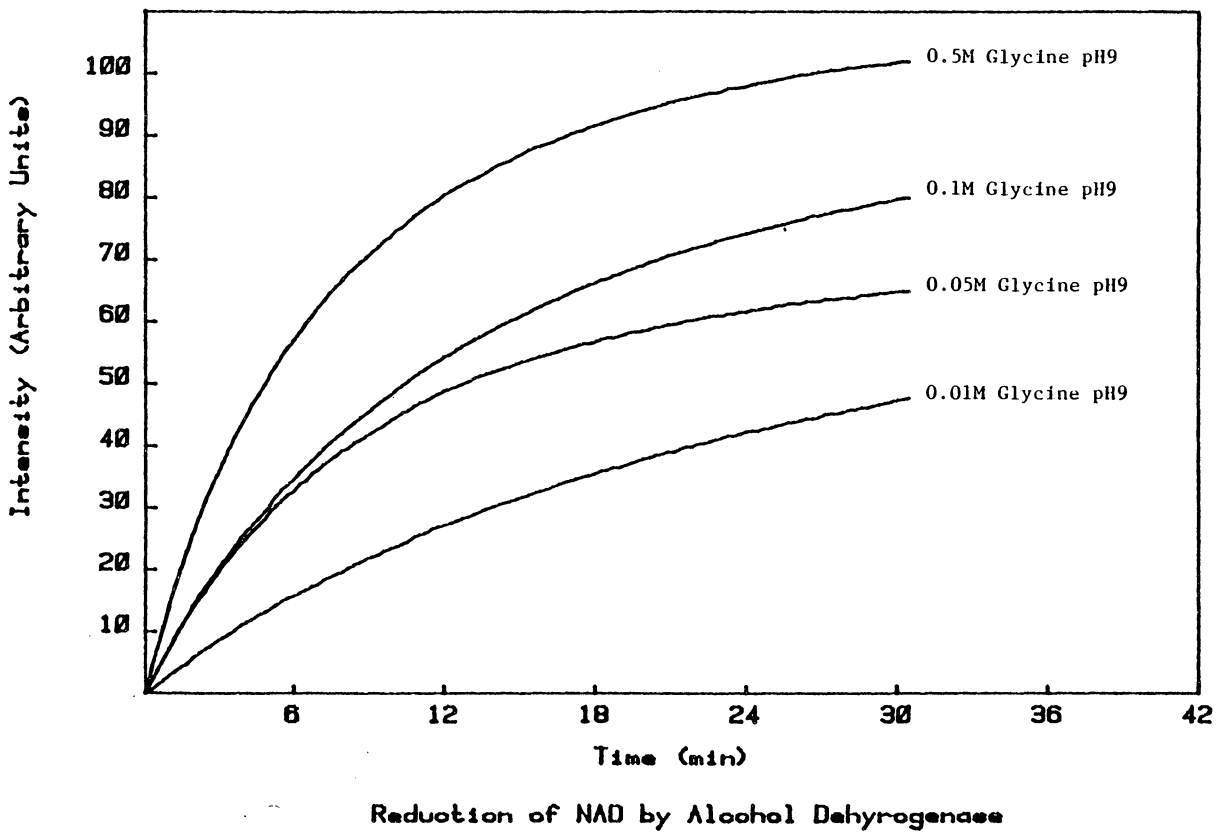

Figure 22. Rate of reduction of NAD^+ by alcohol dehydrogenase in two different buffers at various pHs.

Glucose-6-phosphate dehydrogenase

An alternate enzyme system was saught that favored the reduction of the cofactor. Glucose-6-phosphate dehydrogenase (G-6-PDH) was found to be such a system. This enzyme is supplied in a 3.2M ammonium sulphate solution and has to be reconstituted with a solution which consists of 0.005M glycine and 0.1% bovine serum albumin. A working enzyme solution was prepared by reconstituting 0.25 mL of the G-6-PDH solution with 2.25 mL of the glycine/albumin solution.

A 0.05M Tris buffer containing $5x10^{-4}M$ glucose-6-phosphate and $5x10^{-4}M$ NAD^{+} was placed in the sample beam of the spectrophotometer and 25 microliters of the enzyme solution was added with a micropipette. The absorbance at 340 nm reached its maximum value in about 2 minutes.

To couple the glucose-6-phosphate system to the peroxidase reaction, a reagent stream was prepared which contained $6.25x10^{-5}M$ eosin, $1x10^{-3}M$ Mn^{2+} and 0.15 mg/mL peroxidase. A second solution, comprising $2.5x10^{-4}M$ NAD^{+} and $2.5x10^{-4}M$ glucose-6-phosphate in 0.05 Tris buffer, was injected with 25 microliters of the glucose-6-phosphate dehydrogenase solution. This second solution was allowed

to incubate for about 10 minutes, at room temperature, before injecting into the luminometer. Initially, the G-6-P solution gave quite low light levels. However, subsequent runs gave successively greater light intensities. Presumably, this increasing trend was due to the fact that a steady state NADH concentration had not been reached in the 10 minutes allowed for incubation.

To obtain a more quantitative idea of how long the incubation time should be, the above experiment was repeated but with injections made at exactly 5 minute intervals. Figure 23 shows the system response to incubation time after which a standard incubation time of 30 minutes was selected.

A glucose-6-phosphate working curve was developed by preparing four standard solutions containing various amounts of G-6-P and a constant concentration of NAD^+. A 2.0×10^{-3}M glucose-6-phosphate stock solution was diluted volumetrically to give a range of concentrations between 2×10^{-5}M and 1×10^{-3}M. To each of these standards was added 2 mL of the NAD^+ stock solution to yield a final NAD^+ concentration of 1.1×10^{-3}M. A 25 microliter sample of the enzyme solution was injected into the standards and each was allowed to incubate for 30 minutes before injection into the luminometer. The resulting working curve showed a linear response over almost two orders of magnitude as

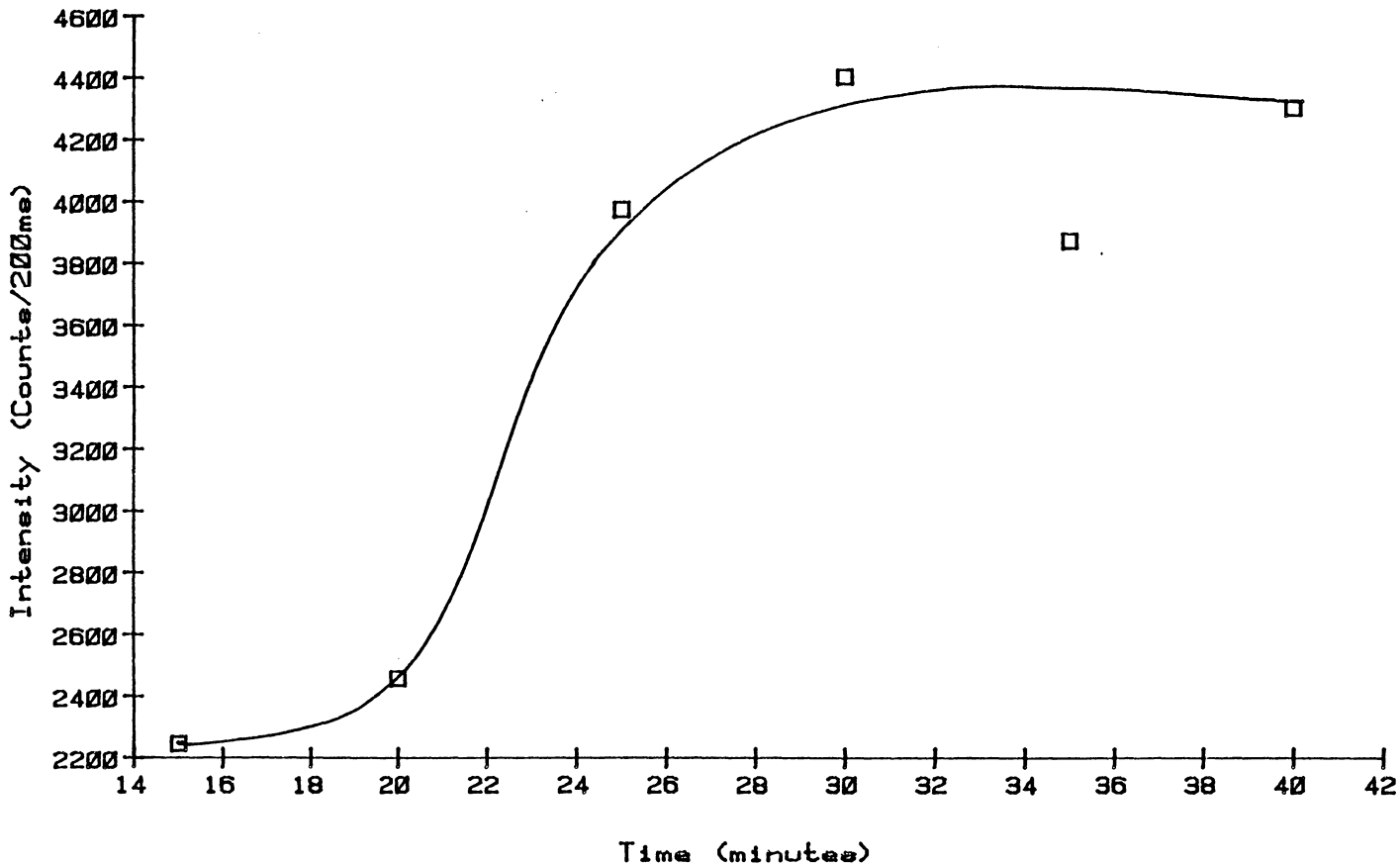

Figure 23. Amount of NAD^+ reduced by glucose-6-phoshate dehydrogenase as a function of incubation time.

can be seen in figure 24. The regression line is: $Y = 4.514 \times 10^{2} + 3.915 \times 10^{7} X$; $r^{2} = 0.997$; $S_{yx} = 9.063 \times 10^{2}$.

Formate dehydrogenase

Another potential enzyme system to couple to the chemiluminescent reaction is formate dehydrogenase. Shaked and Whitesides have reported the following equilibrium constant for the formate reaction (27):

$$K = \frac{[CO_2][NADH]}{[HCO_2^-][NAD^+]} = 10^{5.79} \qquad [8]$$

Because of its favorable equilibrium constant, the suitability of this dehydrogenase was examined further. Five standard solutions were prepared containing formic acid concentrations ranging from 1×10^{-5}M to 1×10^{-3}M. Each solution was also made up to 1×10^{-3}M NAD^+ and 0.3 mg/mL enzyme. The exact compositions of these five standards is described in table 5. The standard solutions were allowed to incubate at room temperature for 30 minutes before being injected into the luminometer. The reagent reservoir was charged with a solution which was 1×10^{-3}M in Mn^{2+}, 6.25×10^{-5}M eosin and 0.23 mg/mL peroxidase. Figure 25 shows the system response to formic acid concentration. The point representing the 1×10^{-5}M standard is not shown

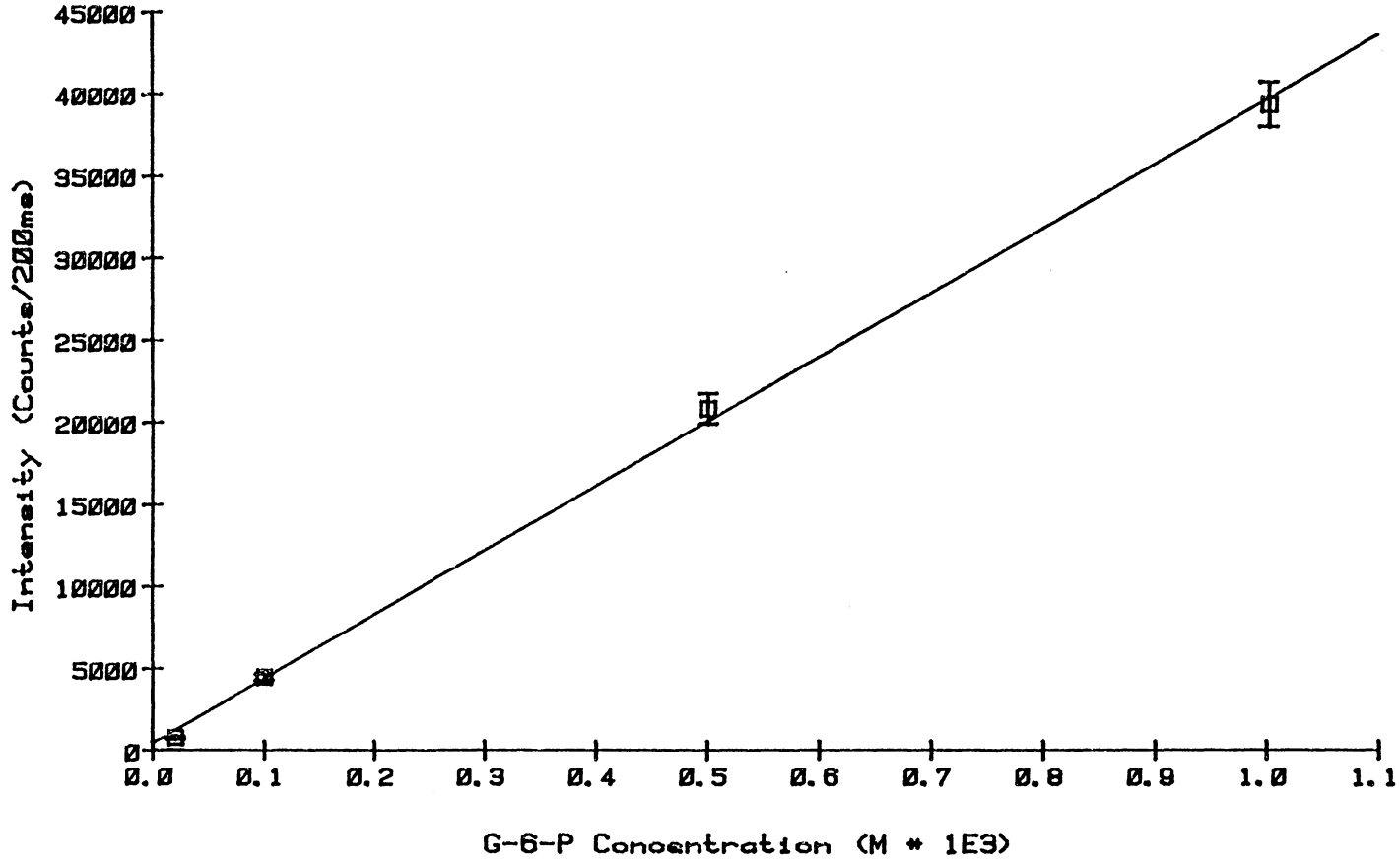

Figure 24. System response to glucose-6-phosphate concentration.

Table 5

Composition of standard solutions used for formic acid calibration curve.

Soln.	Vol. NAD^+	Vol. FDH	Vol. formic acid	final [formic acid]
1	1.0 ml	1.5 ml	0.01 ml	1.06×10^{-5}M
2	1.0 ml	1.5 ml	0.05 ml	5.30×10^{-5}M
3	1.0 ml	1.5 ml	0.10 ml	1.06×10^{-4}M
4	1.0 ml	1.5 ml	0.5 ml	5.30×10^{-4}M
5	1.0 ml	1.5 ml	1.0 ml	1.06×10^{-3}M

NAD^+ stock solution = 1.04×10^{-2}M

Formic acid stock solution = 1.06×10^{-2}M

FDH stock solution = 21.2 mg/ml

Buffer concentration = 0.05M Tris

pH = 7.4

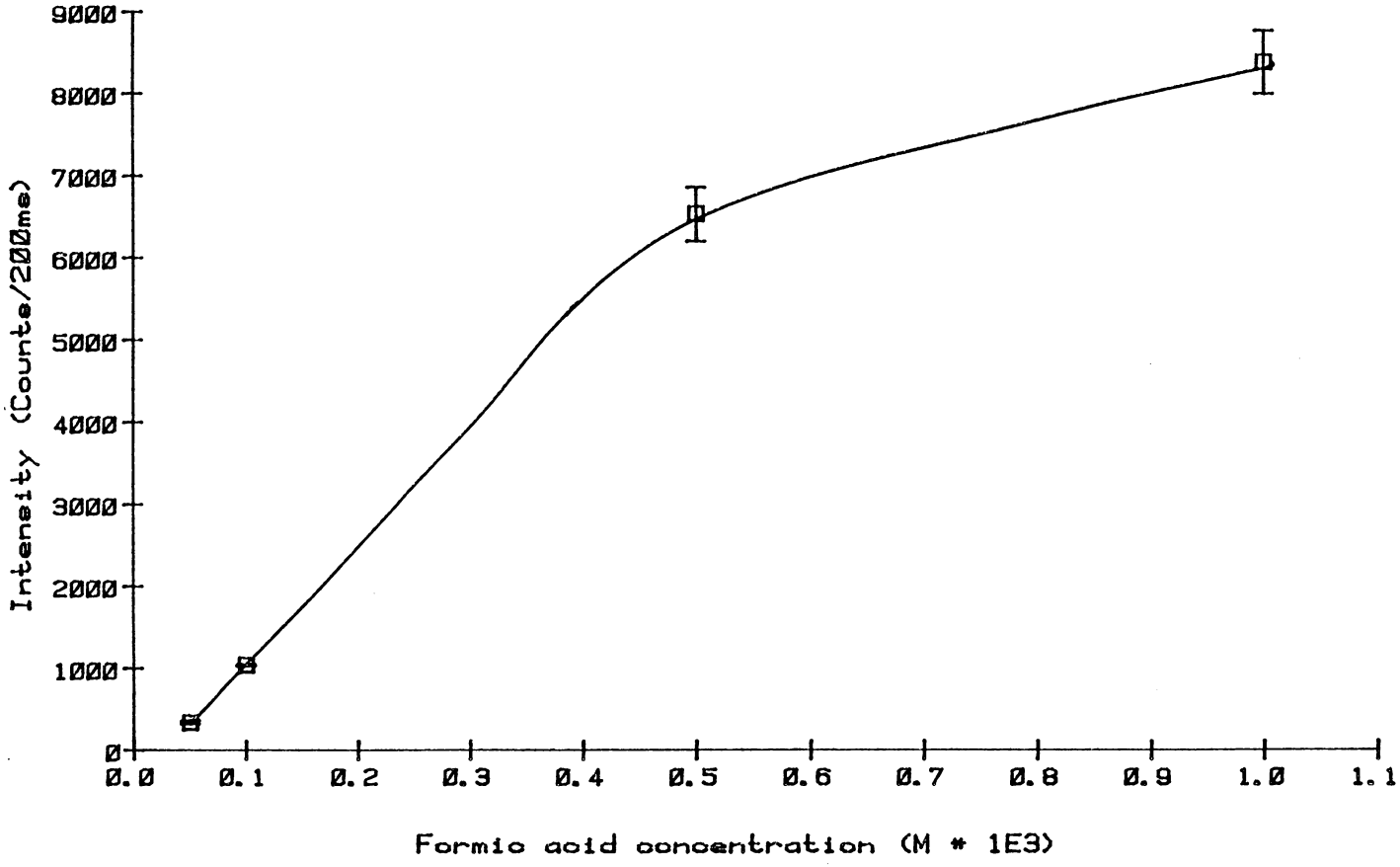

Figure 25. System response to formic acid concentration.

on this plot since the system response for this concentration could not be discerned from the background noise.

Investigation of dye bleaching

If this chemiluminescent reaction is to realize its desired goal the bleaching of the dye, which has been observed thus far, will need to be suppressed. Before any steps can be taken to eliminate this bleaching, the cause will have to be identified. The following section describes those experiments which were carried out in an attempt to pin-point the nature of the bleaching process.

Lactone formation

Looking at the structure of the eosin molecule, attack at carbon atom number 1 would have the most profound effect on the molecule's degree of conjugation. Addition at this site would restrict the delocalization to three isolated benzene rings. The absorption maximum of each isolated ring should be in the 250 nm region which would be out of the visible range. Such an attack would explain the decoloration of the solutions after the reaction is complete.

One means for attack at this position would be the carboxyl group folding back and forming a lactone at this position. This colorless lactone form predominates in strongly acidic solution, while the addition of a base such as KOH or NaOH will regenerate the carboxylate form (28).

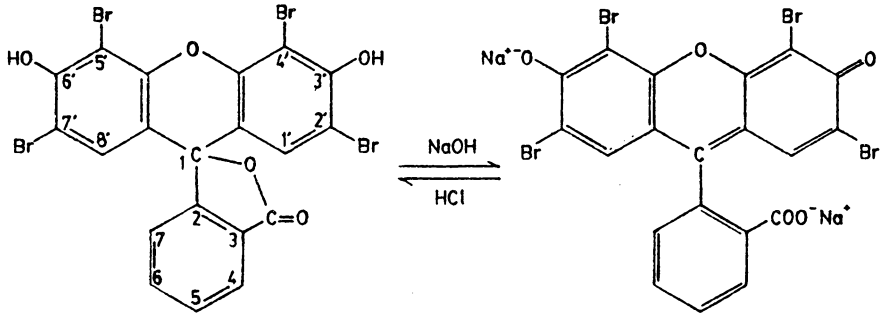

To investigate the possibility of this theory, 2M NaOH was added dropwise to a bleached reaction solution. The optical density of this solution did increase although the newly formed color was more yellow than the original orange. The UV/Visible spectrum of this solution verified that the 518 nm eosin band had not increased noticeably and that a very large, broard band had been introduced beginning below 220 nm and continuing out to just above 600 nm. To identify which of the components of the solution was responsible for this behavior, 2M NaOH was added dropwise to each one of the separate constituents. It was found that the manganese solution was the only one which gave a strong yellow color with the addition of the

base. With the addition of excess base, manganese hydroxide precipitated, therefore, the yellow color is probably due to a mixed chlorohydroxy or perhaps a mixed acetohydroxy complex of manganese.

In another attempt to investigate the possibility of lactone formation, ethyl eosin was substituted for eosin. This molecule has had the carboxy group converted to the ethyl ester and as such should be much less likely to form a lactone.

Since the oxidized form of NAD has a very strong absorption band centered around 260 nm, which might obscure the spectrum of the lactone form of eosin, the bleaching was carried out by the addition of hydrogen peroxide instead of NADH (29).

This ethyl ester of eosin has considerably lower solubility in water, therefore, 1 mg of the dye was dissolved in 200 microliters of ethanol before being diluted to 100 mL with acetate buffer. The resulting solution had a dye concentration of only about 1/10 of that normally used. Consequently, 1 mg of peroxidase was dissolved in 1 mL of 1×10^{-2}M Mn^{2+} solution and diluted to a volume of 10 mL with the ethyl eosin solution. Again the solution took on a more red color as the dye and the enzyme mixed. Three mL of this solution was pipetted into a UV/Visible cuvette and the spectrum of the solution was

recorded before and after the addition of 100 microliters of $1x10^{-2}$M H_2O_2.

As with eosin the ethyl eosin was also bleached by about 50% which would suggest that the bleaching of the dye does not result from eosin's carboxyl group forming a lactone ring at the number 1 position.

Superoxide anion

While the above results suggest that it is not the attack of the number 1 position from the carboxyl group, it does not rule out the possibility of attack from an external agent. Since, in general, peroxidases produce radicals as their products, it would seem reasonable that such a species might be responsible for the attack on the eosin.

The mechanism published by Yokota and Yamazaki (figure 26), describing the oxidation of NADH by peroxidase in the presence of phenols, involves the generation of the superoxide anion from oxygen (20). If this radical was responsible for the bleaching, it should be inhibited by the addition of a large concentration of the enzyme superoxide dismutase. This enzyme is specific for the superoxide anion and dismutes two such radicals into a molecule of oxygen and a molecule of hydrogen

peroxide.

$$2 \cdot O_2^- + 2H^+ \xrightarrow{SOD} H_2O_2 + O_2 \qquad [9]$$

This enzyme will compete for the available supply of $\cdot O_2^-$ and reduce the extent of all reactions involving it. If the bleaching process involves $\cdot O_2^-$ it too should be inhibited to some extent. A 3 mL aliquot of a solution containing 1×10^{-3}M Mn^{2+}, 1.5×10^{-6}M eosin, 0.1 mg/mL peroxidase and 0.05 mg/mL superoxide dismutase was pipetted into a UV/Visible cuvette and the spectrum recorded before and after the addition of 20 microliters of 1×10^{-2}M H_2O_2. Again, the absorbance of the 518 nm band of eosin was reduced by about 50%, which would indicate that $\cdot O_2^-$ is not directly responsible for the bleaching.

Hydroxyl radical

Another highly reactive radical which is often associated with the decomposition of H_2O_2 is the hydroxyl radical $\cdot OH$. In an attempt to scavenge $\cdot OH$ radicals, hydroquinone was added to the reaction mixture. This mixture consisted of 1.5×10^{-6}M eosin, 1×10^{-3}M Mn^{2+}, 0.1 mg/mL peroxidase and 1.5×10^{-6}M hydroquinone. A 3 mL aliquot of this solution was pipetted into a cuvette and the spectrum recorded before and after the addition of 20

microliters of $1x10^{-2}M$ H_2O_2.

The hydroquinone did have a small positive effect on the degree of bleaching, as measured by the intensity of the 518 nm band. Therefore, the concentration of hydroquinone was increased to $1.1x10^{-4}M$ to see if the effect could be increased. At this higher concentration two hydroquinone bands were clearly visible in the absorption spectrum at 245 and 290 nm. After the addition of the H_2O_2 the 518 nm eosin band was observed to decrease by only about 10%. Also, the 290 nm hydroquinone band had decreased in intensity somewhat while the 245 nm band had increased by a factor of approximately five.

While the addition of hydroquinone did help suppress the bleaching of the dye, it also completely suppressed all detectable light output from the system.

EDTA

O'Brien et. al., in their paper describing weak chemiluminescence observed from the action of peroxidase on H_2O_2, in the presence of eosin, mentioned that bleaching of the dye was reduced by the addition of high concentrations of a compound containing a tertiary amine such as EDTA (29). This was a viable solution as their system did not require manganese ions. While it was not

as attractive a solution in the present system, due to EDTA's ability to complex Mn^{2+}, the effect of EDTA was never the less investigated in the absence of Mn^{2+}. A solution containing $1.5x10^{-6}$M eosin and 0.1 mg/mL was bleached by the addition of 20 microliters of $1x10^{-2}$M H_2O_2. The absorption spectrum of this bleached solution was compared with that of a similar solution which also contained $1x10^{-3}$M EDTA. The EDTA did suppress the bleaching to a small extent but not to the extent described by O'Brien.

The most significant observation from this particular experiment was not the effect of the added EDTA, but the effect of the removed manganese. In the absence of manganese, the 518 nm band of eosin almost completely disappeared, whereas in previous experiments its intensity was only reduced by a factor of two. It would appear that the presence of manganese itself prevents a considerable amount of bleaching. If this is indeed the case, increasing the Mn^{2+} concentration still further should have a beneficial effect. When the Mn^{2+} concentration was raised to $9x10^{-3}$M the degree of bleaching was reduced to about 10%, however, as previously noted, increasing the Mn^{2+} to this level suppresses all detectable light output.

DISCUSSION

The oxidation of certain hydrogen donors by horse radish peroxidase, in the presence of phenols, has been under study for many years. Among the most extensively studied donors are indole acetic acid (IAA), NADH and dihydroxyfumarate (DHF) (18,19,20,30,31). The mechanism proposed for the oxidation of these substances, which has been derived from these previous studies, is outlined in figure 26. The following sections draw upon the suggestions of the previous work with conclusions derived from the present study. The results are a better understanding of a complex process.

Initially, the catalyzing phenol (ArOH) is oxidized to a radical (ArO$^{\cdot}$) by the normal action of peroxidase, as depicted in reaction [11]. The H_2O_2 required initially comes from trace quantities naturally present in solution, but it is subsequently provided by reaction [14].

This normal peroxidase reaction can be expressed as the abstraction of a hydride ion from a hydrogen donor, with subsequent reduction of a hydrogen acceptor.

$$2\ RH + H_2O_2 \xrightarrow{HRP} 2\ R^{\cdot} + 2\ H_2O \qquad [10]$$

The enzyme is very non-specific for the hydrogen donor but

$$2\ ArOH + H_2O_2 \xrightarrow{HRP} 2\ ArO^{\cdot} + 2\ H_2O \qquad [11]$$

$$NADH + ArO^{\cdot} \longrightarrow NAD^{\cdot} + ArOH \qquad [12]$$

$$NAD^{\cdot} + O_2 \longrightarrow NAD^{+} + {}^{\cdot}O_2^{-} \qquad [13]$$

$${}^{\cdot}O_2^{-} + NADH + H^{+} \longrightarrow NAD^{\cdot} + H_2O_2 \qquad [14]$$

$$2\ {}^{\cdot}O_2^{-} + 2\ H^{+} \longrightarrow H_2O_2 + O_2 \qquad [15]$$

$$2\ NAD^{\cdot} + H^{+} \longrightarrow NADH + NAD^{+} \qquad [16]$$

Figure 26. Mechanism for the oxidation of NADH by peroxidase in the presence of a phenol.

it fairly specific for the hydrogen acceptor. Hydrogen peroxide is the most effective acceptor for the peroxidase reaction, although other peroxides have been reported.

The next step is the abstraction of a hydride ion from an NADH molecule by the semi-oxidized phenol as illustrated in reaction [12]. The reduced phenol is then free to be reoxidized by the enzyme.

The remaining steps in the oxidation process take the form of a non-enzymic chain reaction described by reactions [13] and [14]. A semi-oxidized NAD molecule can react with dissolved oxygen to produced the fully oxidized NAD^+, with concomitant reduction of the oxygen molecule, (cf. reaction [13]), to yield a superoxide anion. This superoxide anion can then oxidize another NADH molecule to give the semi-oxidized NAD$^\cdot$ and a molecule of H_2O_2. The NAD$^\cdot$ can enter reaction [13], whereas the H_2O_2 can be used to sustain reaction [11].

The chain reaction described by reactions [13] and [14] can be terminated a number of ways. Yamazaki and Piette suggest that two of the most likely chain terminating steps would be the dismutation of the superoxide radical and the dismutation of NAD radicals as illustrated in reactions [15] and [16] (19).

Other chain terminating processes are also possible. One such possibility would be the reaction of the

superoxide anion with peroxidase to yield "Compound III", which is an oxyferroperoxidase (19).

The reaction scheme which has been described thus far does not account for the requirement for manganese ions. Yamazaki and Piette have suggested that the chain terminating dismutation of superoxide anions is fairly rapid and that the Mn^{2+} ions play a role in suppressing this dismutation (19). They have postulated that the Mn^{2+} ions serve as a mediator for the reaction between the superoxide anion and NADH, reaction [14], as follows:

$$\cdot O_2^- + Mn^{2+} + H^+ \longrightarrow H_2O_2 + Mn^{3+} \qquad [17]$$

$$NADH + Mn^{3+} \longrightarrow NAD\cdot + Mn^{2+} + H^+ \qquad [18]$$

Kenten and Mann proposed an alternative role for the manganese ions in the presence of monophenols (32). In their scheme the semi-oxidized phenol, as in reaction [11], was reduced back to the original phenol by its reaction with Mn^{2+} ions.

$$2\ ArOH + H_2O_2 \xrightarrow{HRP} 2\ ArO\cdot + 2\ H_2O \qquad [19]$$

$$ArO\cdot + Mn^{2+} + H^+ \longrightarrow ArOH + Mn^{3+} \qquad [20]$$

They also reported that an excess of Mn^{2+} was inhibitory, which was attributed to the Mn^{2+} competing with the peroxidase for the available H_2O_2.

Effect of pH

The requirement that the chemiluminescent reaction be carried out at a low pH can be possibly accounted for by the formation of an enzyme/dye complex. It was observed in this study, that, after the addition of peroxidase, the enzyme/dye solution at pH 4 developed a more "reddish" color than its pH 5 counterpart. Figure 12 shows the UV/Visible spectra of two such solutions. These two spectra reveal that the main 518 nm band of eosin has suffered the greatest percentage reduction in intensity.

The work of a number of authors has suggested that the 518 nm chromophore can be attributed to the para-quinoid structure of the eosin molecule (33,34). Disruption of this delocalized quinoid structure would result in a decrease of the 518 nm band. In strongly acidic media, for example, the quinoid structure of eosin is destroyed by the formation of a lactone (28). This lactone formation isolates all three aromatic rings to yield a colorless molecule.

The experimentally observed behavior (figure 12) suggests, therefore, that the interaction between the dye and the enzyme is effecting the quinoid structure to some extent. The results of a related experiment undertaken

during this study also indicates that the carboxy group is not likely to be the point of complexing with the enzyme. When peroxidase was added to a solution of ethyl eosin, an ethyl ester of eosin, the same color change was observed at pH 4. Therefore, it would seem that the most probable site for complexing with the enzyme is the phenoxy group.

The dependance of the reaction on the buffer concentration discovered in this study, as illustrated in figure 13, may be the result of an enzymatic sensitivity towards the ionic strength of the reaction medium. Variations in enzyme performance as a result in variations to ionic strength are quite common in biochemical reactions. Such an effect can be seen, for alcohol dehydrogenase, in figure 22. An alternative interpretation may be that one of the reactions in the light emitting process is acid catalyzed, although it is not clear at this point which specific reaction would be sensitive to such acid catalysis.

Mn^{2+} concentration

Figure 14 shows the system response to manganese concentration as studied in the current work. The maximum that this response curve goes through may the result of two effects. Yamazaki and Piette suggested that a

possible role for the manganese ions is to prevent the dismutation of $^{\cdot}O_2^-$ and thus propagate the chain reaction described by equations [13] and [14]. Therefore, at low Mn^{2+} concentrations this chain reaction may be slowed by dismutation and the rate of generation of H_2O_2 would be reduced. A reduced rate of H_2O_2 production would also have a negative effect on the rate of reaction [11] which is associated with the light emitting process. Since the intensity of a signal from the pulse counting detector is a measure of the photon flux, or the number of photoelectric events per unit time, a reduction in the rate of the light emitting reaction would result in a reduced signal.

Kenten and Mann concluded that at higher manganese concentrations there could be effective competition between peroxidase and the Mn^{2+} ions for the available H_2O_2 (32). Direct reaction between the generated H_2O_2 and manganese would inhibit reaction [11] but would not effect the chain reaction. This would explain the reduced light intensity at higher Mn^{2+} concentrations.

Peroxidase concentration

The first step in the oxidation of NADH has been proposed to be the formation of a dye radical by the

oxidation of a dye molecule via peroxidase. Therefore, it would seem reasonable that the signal should be proportional to the enzyme concentration. This would certainly be true while the enzyme concentration is sufficiently low that the enzyme remains saturated. In this instance the enzyme's turnover number limits the rate of the reaction. However, as the enzyme concentration rises to the point where not all of the active sites are saturated the substrate concentration controls the rate of the reaction. This effect can be obtained from the Michaelis-Menton equation.

Consider a general enzyme process:

$$E + S \underset{k_2}{\overset{k_1}{\rightleftharpoons}} ES \xrightarrow{k_3} E + P \qquad [21]$$

Where E is the enzyme, S is the substrate, ES is the enzyme/substrate complex and P is the product. The Michaelis-Menton equation for such a process is:

$$\text{Rate} = k_3[E_{total}] \frac{[S]}{[S] + K_m} \qquad [22]$$

When the substrate concentration is very high, relative to the enzyme concentration, the term $[S]/([S] + K_m)$ approaches unity. In this case the rate of the reaction should be proportional to the enzyme concentration. This

can be seen in figure 15, which is derived from the present work, for those enzyme concentrations below 0.1 mg/mL. Above 0.1 mg/mL the enzyme's active sites are presumably not fully saturated, in which case the $[S]/([S] + K_m)$ term starts to become dominant.

With the constant substrate concentration used in this work, one would expect the signal, above 0.1 mg/mL, to also remain constant. However, as can be seen from figure 15, there is a decrease in response at 0.2 mg/mL. This decrease in intensity could be attributable to an effect that was observed by Kenten and Mann (32). They suggested that excess peroxidase can complex with $^{\cdot}O_2^-$ to form an oxyferroperoxidase known as "Compound III". If excess peroxidase begins to compete for $^{\cdot}O_2^-$, the chain reaction would be inhibited, which would in turn inhibit the oxidation of the dye and therefore reduce the light output.

Eosin concentration

From reactions [11] and [12] it can be seen that the catalyzing phenol should be recyclable. One would therefore expect the system response to be somewhat independant of the dye concentration. However, as can be seen from figure 16, which is derived from this work, the

response increases with increasing dye concentration. This curve, in fact, resembles a Michaelis-Menton plot for a normal enzyme/substrate reaction. This would imply that the eosin, which is acting as the substrate for peroxidase, is being irreversibly oxidized by the enzyme. The nature of this oxidized product is not clear, although some form of oxygenated dye molecule is likely. Hydroxylation of aromatic substrates is well known for certain classes of enzymes known as "oxygenases". An oxygenase activity has been suggested as a possible alternative mechanism for peroxidase during the oxidation of IAA (31).

Oxygen requirement

There is some debate in biochemical circles as to the exact sequence of events associated with this oxygenation (35). One point of moderate agreement seems to centered around the formation of an ESO_2 ternary complex. The nature of the oxygen also seems to differ depending upon the particular enzyme system in question. In some instances it appears to be molecular oxygen, in others it appears to be the superoxide anion and in others it is believed to be derived from H_2O.

It was found experimentally, during this study, that when peroxidase was added to an acetate buffer solution containing eosin and Mn^{2+}, there was a very distinct color change from orange to red-orange. This would imply that there is some sort of enzyme complex being formed. If nitrogen is bubbled through the solution for about fifteen minutes, the red-orange color disappeares leaving the original orange color of the eosin/Mn^{2+} solution. The red-orange color does not immediately return if oxygen is then bubbled through the deoxygenated solution. However, it was noticed that the red-orange color did return if the solution was let stand over night. This behavior would suggest that oxygen is somehow associated with the enzyme/dye complex. It may be that the red-orange color results from a peroxidase-eosin-O_2 ternary complex.

It was found that addition of oxygen to the enzyme/dye/Mn^{2+} and NADH solutions depressed the intensity of the luminescence peaks as can be seen in figure 18. The question that arises is whether this added oxygen is interfering with the enzyme/dye complex or whether it is inhibiting some other aspect of the process.

If the enzyme/dye complex is indeed a ternary complex involving O_2 it would seem unlikely that additional oxygen would have a marked inhibitory effect upon its performance.

As can be seen from figure 26, reaction [13] requires molecular oxygen. The addition of oxygen may speed up the chain reaction of reactions [13] and [14]. The light emitting reaction, proposed by Cilento et. al., is the interaction of an eosin radical with an NAD radical (6).

$$\text{eosin}^{\cdot} + \text{NAD}^{\cdot} + \text{H}^{+} \text{------>} [\text{eosin}]^{*} + \text{NAD}^{+} \qquad [23]$$

$$[\text{eosin}]^{*} \text{------>} \text{eosin} + \text{light} \qquad [24]$$

An increase in the rate of the chain reaction would leave less NAD radicals available to participate in the luminescent process and therefore reduce the overall peak intensity.

Eosin bleaching

Because of the bleaching of the dye that occurs as a result of the light emitting process, this particular chemiluminescent reaction did not realize the initial goal of a recycling luminescent process. Two steps were, however, somewhat successful in reducing the amount of bleaching: (1) the addition of excess Mn^{2+} and (2) the addition of hydroquinone. Both steps, unfortunately, also quenched the luminescent reaction. The effect of a relatively good radical scavenger such as hydroquinone implies that the bleaching process may be a radical

reaction. However, it does not give any information on the nature of the reaction.

The dismutation of superoxide anions has already been discussed as a chain terminating step and the addition of Mn^{2+} ions has been suggested as a means of reducing that rate of dismutation. If the bleaching process is the result of the reaction of eosin radicals and superoxide anions, then Mn^{2+} ions would perhaps be expected to inhibit the bleaching process. Unfortunately, the addition of superoxide dismutase to the reaction mixture did not confirm that the superoxide anion is responsible for the bleaching.

NADH response

Despite the fact that recyclability doesn't appear a reality, the chemiluminescent reaction does show a linear response to NADH over a two order of magnitude concentration range. The minimum detectable quantity was calculated to be $1x10^{-6}M$ which is competitive with absorption methods, which are useful down to the $1-5x10^{-6}M$ range (36). Traditionally, luminescence methods have been capable of greater sensitivity than absorption methods. However, in this particular case only a fraction of the NADH is being channeled into the emitting process thus

reducing the overall luminous output. Because of this relatively low light level it is unlikely that this particular chemiluminescent reaction will supplant the absorption methods.

Since NAD^+ is a cofactor for many enzyme reactions, they should be able to be coupled to the chemiluminescent reaction to obtain a luminescence signal proportional to substrate concentration. Those reactions which favor the reduction of NAD^+ to NADH have proven to be the most viable due to their lower pH requirements.

Glucose-6-phosphate response

Glucose-6-phosphate dehydrogenase was found to be such an enzyme system that reduces NAD^+ and which can be run at a neutral pH. Because of these favorable conditions this enzyme system has been successfully coupled to the chemiluminescent reaction. This pair of reactions was found to give a linear response to glucose-6-phosphate over a two order of magnitude concentration range (figure 24). The requirement for a 30 minute incubation period is not unusual in enzyme analyses. This incubation time could possibly be reduced by the addition of a trapping agent for the 6-phosphogluconate which is a product of the first

reaction.

Glucose-6-phosphate dehydrogenase is an interesting enzyme because it can be coupled with hexokinase to produce an analysis for glucose.

$$\text{glucose} + \text{ATP} \xrightarrow{\text{HK}} \text{G-6-P} + \text{ADP} \qquad [25]$$

$$\text{G-6-P} + \text{NAD}^+ \xrightarrow{\text{G-6-PDH}} \text{6-PG} + \text{NADH} \qquad [26]$$

The NADH produced by these two reactions could then be analyzed with the chemiluminescent reaction to give a luminescent signal proportional to the glucose concentration. The range of linearity observed for the chemiluminescent system corresponds fairly well within the normal levels of glucose found both in serum and urine. Unfortunately, a very strong competitor for the chemiluminescent analysis of serum glucose is glucose oxidase coupled with the luminol reaction. Considering the much higher light output of the luminol reaction, it would probably turn out to be the reaction of choice.

Formate response

Another enzyme system that was tried was formate dehydrogenase. At low substrate concentrations it did exhibit a linear response, although at high substrate

concentrations the response rolled off from linearity quite badly. The exact cause of this non-linearity is not clear at this point. One possible explanation could be the inhibition of the enzyme by excess product. This particular effect is not uncommon in biochemical reactions, with the firefly enzyme, luciferase, being a classic example. The reasonably high solubility of CO_2 would allow a considerable accumulation of this product in solution, therefore, posing a potential inhibition problem. This problem of product inhibition could perhaps be helped by the addition of a trapping agent for the product molecule.

Even though the response to formate concentration has been observed to be non-linear, this is not to say that it cannot be analytically useful. The non-linearity simply means that a larger number of standards would be needed to characterize the shape of the curve. This would particularly apply to the point on the curve where the slope changes sharply.

SUMMARY

The purpose of this research was to investigate the chemiluminescent oxidation of NADH by horse radish peroxidase in the presence of eosin. This particular reaction was chosen because it appeared to possess the property of a recycling luminescing species. Such a reaction merited investigation because it would provide the first essential step necessary for the design of a chemiluminescent probe that could be reuseable or would be applicable to continuous monitoring.

An automated luminometer was designed and constructed to facilitate the investigation of reaction conditions and to test the reaction's analytical viability. A fully automated delivery system was provided for the injection of the sample, addition of reagents and the rinsing of the system after a run. In addition to the reduction in sample handling that was necessary, the automated injection system also provided increased reproducibility over manual syringe injection. A pulse counting detector system was used to provide improved sensitivity and signal to noise ratio.

Each one of the major reaction parameters was investigated individually in order to obtain insight into the most favorable conditions under which to run the reaction. The optimized conditions correspond to a pH of

4, enzyme concentration of 0.1 mg/mL, manganese concentration of $5x10^{-4}M$ and an eosin concentration of $5x10^{-5}M$.

During the course of the investigation it became apparent that the eosin was being bleached. The bleaching process was examined in order to learn what was causing it and then take steps to prevent it. It soon became apparent that those techniques that were successful at reducing the degree of bleaching also quenched the chemiluminescence. It is postulated that the bleaching is a result of the reaction of eosin radicals and some form of oxygen, perhaps the superoxide anion. Because of the severe degree of bleaching that occurs at high NADH concentrations it is unlikely that substantial recycling of the dye is possible.

Despite the lack of recyclability, this chemiluminescent reaction has proven to be a successful analytical probe for the determination of NADH. The response to NADH concentration is linear over two orders of magnitude between $5x10^{-6}M$ and $5x10^{-4}M$ with a calculated limit of detection of $1x10^{-6}M$. This compares quite favorably with established absorption techniques. The analysis time is quite short, approximately three minutes, and the average reproducibility is 5% RSD.

Because NAD^+ is such a ubiquitous cofactor amongst biochemical reactions, the chemiluminescent reaction should be able to be used as an indirect sensor for the substrates of these biological reactions. Glucose-6-phosphate dehydrogenase has been successfully coupled to the chemiluminescent reaction for the determination of glucose-6-phosphate. Again response was linear over approximately two orders of magnitude between $1x10^{-5}M$ to $1x10^{-3}M$ with better than 5% RSD reproducibility.

Another biochemical system that was chosen for coupling to the chemiluminescent reaction was formate dehydrogenase. This particular system provided only about one order of magnitude of linearity, between $5x10^{-5}M$ and $5x10^{-4}$, with the response levelling off at formate concentrations above $5x10^{-4}M$. This levelling off could be due to product inhibition of the enzyme at high substrate concentrations. Even though the response curve is not linear over a wide range the method could serve as an analytical approach provided that sufficient calibration points were available to define the shape of the non-linear function.

In conclusion, it does not appear that this particular chemiluminescent reaction will serve as the first step in the design of a reuseable or continuous

chemiluminescent monitor. However, it has provided a chemiluminescent method for the determination of NADH which is simple, rapid and competitive with existing absorption techniques in terms of sensitivity.

However, before chemiluminescent methods can realistically take over from the absorption techniques for the determination of NADH, the chemiluminescent reaction employed must have a high luminescence efficiency and utilize inexpensive, stable reagents. Firefly luciferase as well as a number of bacterial luciferases have very high quantum efficiencies and have been adapted to to the determination of NADH, but they are still too expensive to be competitive.

For the purpose of a reuseable or continuous chemiluminescent monitor, one of the flavine mononucleotide oxidoreductases from a luminous bacteria such as Beneckea harveyi may be another promising candidate (37). These enzymes reduce FMN to $FMNH_2$ with concomitant oxidation of NADH to NAD^+. The reduced $FMNH_2$ can be reoxidized by firefly luciferase in the presence of decanal and O_2 to yield chemiluminescence. This type of reaction sequence is now becoming more practical with the recent commercial availability of the bacterial NADH:FMN oxidoreductases.

REFERENCES

1. Hercules, D. M. Acct. Chem. Res. 1969, 2, 301-307.

2. Albrecht, H. O. Z. Physik. Chem. 1928, 135, 321-330.

3. Seitz, W. R.; Neary M. P. Anal. Chem. 1974, 46(2), 188A.

4. Simpson, J. S. A.; Campbell, A. K.; Woodhead, J. S.; Richardson, A.; Hart, R.; McCapra, F. In "Bioluminescence and Chemiluminescence : Basic Chemistry and Analytical Applications"; DeLuca, M. A.; McElroy, W. D.; Eds.; Acedemic Press: New York, 1981; pp 673-679.

5. Freeman, T. M.; Seitz, W. R. Anal. Chem. 1978, 50(9), 1242-1246.

6. Kachar, B.; Zinner, K.; Vidigal, C. C. C.; Shimizu, Y.; Cilento, G. Arch. Biochem. Biophys. 1979, 195(1), 245-247.

7. Seitz, W. R.; Suydam, W. W.; Hercules, D. M. Anal. Chem. 1972, 44(6), 957-963.

8. Seitz, W. R.; Hercules, D. M. Anal. Chem. 1972, 44(13), 2143-2149.

9. Olsson, T.; Bergstrom, K.; Thore, A.; "Bioluminescence and Chemiluminescence", (Academic Press, 1981) pp 659-665.

10. Shaw, F. Analyst 1980, 105, 11-17.

11. Auses, J. P.; Cook, S. L.; Maloy J. T. Anal. Chem. 1975, 47(2), 244-249.

12. Bostick, D. T.; Hercules D. M. Anal. Chem. 1975, 47(3), 447-452.

13. Branchini, B. R.; Hermes, J. D.; Salituro, F. G.; Post, N. J.; Claeson, G. Anal. Biochem. 1981, 111, 87-96.

14. Ikariyama, Y.; Aizawa, M.; Suzuki, S. J. Solid-Phase Biochem. 1980, 5(4), 223-233.

15. Lee, Y.; Jablonski, I.; DeLuca, M. Anal. Biochem. 1977, 80, 496-501.

16. Lippman, R. D. Anal. Chim. Acta. 1980, 116, 181-184.

17. Vogelhut, P. O. US Patant No. 4,231,754, Nov. 4, 1980.

18. Akazawa, T.; Conn, E. E. J. Biol. Chem. 1958, 232, 403-415.

19. Yamazaki, I.; Piette, L. H. Biochim. Biophys. Acta. 1963, 77, 47-64.

20. Yokota, K.; Yamazaki, I. Biochim. Biophys. Acta. 1965, 105, 301-312.

21. Arrio, B.; Lecuyer, B.; Dupaix, A.; Volfin, P.; Jousset, M.; Carrette, A. Biochimie 1980, 62, 445-453.

22. Zinner, K.; Personal communication, (December, 1982).

23. "Handbook of Chemistry and Physics", 59th edition; Weast, R. C. Ed.; CRC Press: Boca Raton, 1978-1979; p C-284.

24. Graichen, C.; Molitor, J. C. J.A.O.A.C. 1959, 42(1), 149-160.

25. Marshall, P. N.; Lewis S. M. Stain Technology. 1974, 49(4), 235-240.

26. Hammett, L. P. In "Physical Organic Chemistry"; McGraw-Hill: New York, 1940; pp 330-336.

27. Shaked, Z.; Whitesides, G. M. J. Amer. Chem. Soc., 1980, 102, 7105-7107.

28. Lillie, R. D. In "H. J. Conn's Biological Stains", 9th edition; Williams and Wilkins: Baltimore, 1977; p 335.

29. O'Brien, P. J.; Bechara E. J. H.; O'Brien C. R.; Duran, N.; Cilento, G. Biochem. Biophys. Res. Comm. 1978, 81(1), 75-81.

30. Kalyanaraman, V. S.; Kumar, S. A.; Mahadevan, S. Biochem. J. 1975, 149, 577-584.

31. Yamazaki, I. In "Molecular Mechanisms of Oxygen Activation"; Hayaishi, O. Ed.; Acedemic Press: New York, 1974; pp 539-544.

32. Kenten, R. H.; Mann, P. J. G. Biochem. J. 1950, 46(1), 67-73.

33. Grzywacz, J.; Smagowski, H. Z. Naturforschung 1965, 20a, 1358-1363.

34. Nagase, T.; Ohno, T.; Goto, T. J. Pharm. Soc. Japan., 1951, 73, 1033-1039.

35. Hayaishi, O. In "Molecular Mechanisms of Oxygen Activation"; Hayaishi, O. Ed.; Acedemic Press: New York, 1974; pp 1-28.

36. Nisselbaum, J. S.; Green, S. Anal. Biochem. 1968, 27, 212-217.

37. Jablonski, E.; DeLuca, M. Clin. Chem. 1979, 25(9), 1622-1627.

38. Marshall, P. N.; Bentley, S. A.; Lewis, S. M. Stain Technology. 1975, 50(2), 107-113.

APPENDIX A

SOFTWARE GLOSSARY

FORTH WORD	TYPE	BLOCK	STACK
MEAN	COLON	292	(addr count -- mean)

Takes the arithmetic mean of a list of floating point numbers which begins at 'addr' and is 'count' numbers in length. The floating point mean is returned on the stack.

VARIANCE	COLON	292	(addr count -- variance)

Calculates the variance of a list of 'count' floating point numbers stored in memory starting at address 'addr'. The floating point variance is returned on the stack.

STD.DEV	COLON	292	(addr count -- std.dev)

Returns, on the stack, the floating point standard deviation of the series of 'count' floating point numbers in memory starting at address 'addr'.

SCOPE-TASK	TASK	308	(-- addr)

SCOPE-TASK is the multiprogrammed task which provides a continuous XY oscilloscope display of a data set.

0DAC	CONST	308	(-- addr)

A mnemonic constant which returns the address of DAC 0

1DAC	CONST	308	(-- addr)

A mnemonic constant for the address of DAC 1.

DATA-ADDR	VARIABLE	308	(-- addr)

A variable which is used to transmit the address of the data array to be displayed from the terminal task to the scope task.

#POINTS	VARIABLE	308	(-- addr)

A variable which is used to pass the length of the data array to the scope task from terminal task.

1SCAN CODE 308 (addr count --)

Outputs the contents of a 16 bit integer data array to an XY oscilloscope, once, as fast as possible. As each datum is transmitted to the DAC it is scaled by a factor of 0.06247 to prevent the display from wrapping prematurely.

SCOPE COLON 308 (addr count --)

Initiate the repetitive XY display of a 16 bit integer data array on an oscilloscope. This routine calls 1SCAN on every third tick of the 60 Hz clock to keep the screen refreshed.

SUSPEND COLON 308 (task --)

This definition is used to suspend an active task. It assumes that there are no special task shut down procedures such as the disabling of hardware interrupts. The task is disabled by simply forcing it to execute STOP the next time the task is activated. SUSPEND is usually used to kill a task which has been activated erroneously.

TICKS/DATUM VARIABLE 309 (-- addr)

This variable hold the number of clock B ticks which must occur before the counter is read. Since the Conder clock can only produce frequencies which are powers of ten, this variable provides a simple yet flexible means of synchronizing data acquisition at frequencies which are not powers of ten.

ELAPSED-TICKS VARIABLE 309 (-- addr)

ELAPSED-TICKS is the variable which hold the number of ticks which have to occur before the counter is read. When ELAPSED-TICKS has been decremented to zero the counter is read and ELAPSED-TICKS is reset to the value of TICKS/DATUM.

<PC-EXPECT> ISR 309 (-- addr)

<PC-EXPECT> is not a user executable definition, but is the interrupt service routine (ISR) for the pulse counting clock. This interrupt service routine is responsible for fielding all clock B

interrupts, deciding if the counter is to be read on a particular interrupt, reading the counter and returning the count to the pulse counting task. The address of <PC-EXPECT> is loaded into the input ISR cell of PC-TASK's user table so that when a clock B interrupt occurs it vectors directly to PC-TASK's user table. This eliminates the need for a clock B semaphore.

PC-TASK TASK 314 (-- addr)

This is the name of the multiprogrammed task which is responsible for the control of the pulse counting system.

(ACQUIRE) COLON 315 (addr count --)

This definition is the main routine which initiates and controls the data acquisition. It instructs PC-TASK to switch the sample loop into the inject position, enable the pulse counting clock and begin waiting for counts to be returned from the interrupt service routine. Once 60 points have been collected, the valve control is instructed to inject the sample and then the rest of the data is collected.

ACQUIRE COLON 315 (addr count --)

ACQUIRE is the main definition with which the operator interacts. It is essentially just a rename of (ACQUIRE) but clears the data array first.

PCSR CONST 319 (-- addr)

A mnemonic constant for the address of the parallel board.

ACLK.CSR CONST 319 (-- addr)

A mnemonic constant for the address of clock A.

BCLK.CSR CONST 319 (-- addr)

A mnemonic constant for the address of clock B.

DCLK.CSR CONST 319 (-- addr)

A mnemonic constant for the address of clock D.

ACLOCK VARIABLE 319 (-- addr)

A semaphore used to contain the user table address of the task currently using clock A. When clock A is not in use this variable contains zero.

VALVES VARIABLE 319 (-- addr)

This variable is a semaphore which is used to coordinate the concurrent operation of the clock A and clock D interrupt service routines and the valve control task. When a sample is injected the two Series 9 valves have to be open simultaneously which requires both clock A and clock D to be enabled together. While both valves are open VALVES has a value of 2. When each of the two interrupt service routines recognize that it's time to close its respective valve each ISR will decrement VALVES. Whichever ISR decrements VALVES to zero is then the ISR responsible for reactivating the valve control task.

1VALVE VARIABLE 319 (-- addr)

1VALVE is the variable which contains the bit mask which the clock A interrupt service routine uses to tell which valve is to be controlled by clock A.

2VALVE VARIABLE 319 (-- addr)

Similar to 1VALVE, this variable contains the bit mask which the clock D ISR uses to tell which valve to open.

DAT-ADDR VARIABLE 319 (-- addr)

This variable contains the absolute memory address of the most recently stored datum. When the VALVE-TASK is instructed by the PC-TASK to inject the sample, the value pointed to by DAT-ADDR is multiplied by 2 to give an injection point marker in the data set.

no name ISR 319 (--)

Lines 8 to 13 in block 319 define the clock A interrupt service routine.

D.CNT VARIABLE 320 (-- addr)

This variable serves as a flag to indicate to the clock D ISR when to begin acknowledging interrupts. When the interrupt enable bit is set, an interrupt occurs immediately. The time interval between this interrupt and the next interrupt does not necessarily represent one complete clock period. Consequently, D.CNT is initialized to -2 and is incremented each time an interrupt occurs. Once D.CNT has been incremented to zero the clock D ISR opens the valve and begins counting interrupts.

D.CNTR VARIABLE 320 (-- addr)

D.CNTR holds the number of milliseconds for which the valve, being controlled by clock D, is to be held open. This variable is decremented on each interrupt and when it has been decremented to zero the ISR is responsible for closing the valve. The two variables D.CNT and D.CNTR are directly analogous to the user table variables CNT and CTR. VALVE-TASK's user table variables are unavailable to the clock D ISR because they are always used by the clock A ISR.

no name ISR 320 (--)

Lines 4 to 10 of block 320 define the clock D interrupt service routine.

(VALVE-ON) CODE 321 (mask1 time1 mask2 time2 --)

This routine is called by the valve control task to set up the masks and times for a particular valve operation, enables the appropriate clock(s) and then suspends the task until the valve operation is complete.

VALVE-ON COLON 321 (mask1 time1 mask2 time2 --)

VALVE-ON is just a high level version of (VALVE-ON) which also stores the address of VALVE-TASK's user table into the semaphore ACLOCK. Without this address the interrupt service routines would not know which task to reactivate after the completion of a valve operation.

MIX COLON 321 (--)

Mixes the sample and the reagent streams by simultaneously opening the two Series 9 valves.

INJECT COLON 321 (--)

Switch the sample loop into the inject position.

FILL COLON 321 (--)

Switch the sample loop back into the load position.

WASH COLON 321 (--)

Open the sample stream injection valve to fill the cell with clean acetate buffer.

DRAIN COLON 322 (--)

This definition is the one used to drain the cell of spent reactants. It could not be defined in terms of VALVE-ON because it requires three valves to be open simultaneously. Draining of the cell is not a time critical operation, therefore, it could be synchronized with the 60 Hz day clock.

VALVE-TASK TASK 322 (-- addr)

This is the multiprogrammed task which supervised the operation of all of the valves.

RINSE COLON 323 (--)

RINSE performs a complete rinse of the cell by draining, washing and redraining the cell.

LOAD-POSN COLON 323 (--)

A definition executed by PC-TASK to instruct VALVE-TASK to switch the sample loop into the load position.

INJECT-MARK COLON 323 (--)

INJECT-MARK is executed by VALVE-TASK to induce the injection point marker into the data set by doubling the datum pointed to by the variable DAT-ADDR.

INJECT-SAMPLE COLON 323 (--)

This definition is executed by PC-TASK and it instructs VALVE-TASK to inject the sample into the cell.

RINSE-CELL COLON 323 (--)

RINSE-CELL is executed by PC-TASK to indicate to VALVE-TASK that the data acquisition is complete and that it should now rinse the cell. to inject the sample into the cell.

TAREA VARIABLE 325 (-- addr)

This is a floating point variable which holds the accumulated area during the integration of a peak.

BASELINE VARIABLE 325 (-- addr)

A floating point variable which hold the mean of the first 60 baseline values.

HEIGHT VARIABLE 325 (-- addr)

A floating point variable used in searching for the maximum value in a data array.

HEIGHTS COLON 325 (addr --)

Scans through a data array, calculates the mean baseline value, subtracts this mean baseline from the maximum value in the array to yield a corrected peak height and integrates the area of the peak.

PSHOW COLON 325 (sblk# eblk# --)

Analyses a series of spectra which are stored contiguously, starting at block 'sblk#' and ending at block 'eblk#'.

APPENDIX B

SOFTWARE LISTINGS

```
291 LIST

 0 ( EMPTY )
 1
 2
 3
 4
 5
 6
 7
 8
 9
10
11
12
13
14
15

292 LIST

 0 ( SIMPLE STATS STUFF        9/30/83)
 1
 2 : MEAN  ( addr count -- mean)
 3      0.  2SWAP  DUP >R  4*  OVER + SWAP DO  I 2@  F+  4 +LOOP
 4      R> 0 FLOAT  F/ ;
 5
 6 : VARIANCE   ( addr count -- variance)
 7      >R >R  0. ( SIGMA[X**2])   0. ( SIGMA[X])
 8      R> I 4*   OVER + SWAP  DO  I 2@ ( X)  2DUP 2DUP F* ( X**2)
 9      'S 12 +  F+!   'S 4 + F+!   4 +LOOP
10      2DUP F*  I 0 FLOAT  F/  F-   R> 1- 0 FLOAT  F/  ;
11
12 : STD.DEV   ( addr count -- std.dev)   VARIANCE  SQRT ;
13
14
15

293 LIST

 0 ( EMPTY )
 1
 2
 3
 4
 5
 6
 7
 8
 9
10
11
12
13
14
15
```

```
306 LIST

 0 ( EMPTY )
 1
 2
 3
 4
 5
 6
 7
 8
 9
10
11
12
13
14
15

307 LIST

 0 ( EMPTY )
 1
 2
 3
 4
 5
 6
 7
 8
 9
10
11
12
13
14
15

308 LIST

 0 ( SCOPE DISPLAY TASK)            OCTAL
 1 177560 160 300 TERMINAL SCOPE-TASK   SCOPE-TASK CONSTRUCT
 2 176760 CONSTANT 0DAC      0DAC 2 +  CONSTANT 1DAC
 3 VARIABLE DATA-ADDR        VARIABLE #POINTS
 4
 5 CODE 1SCAN    ( addr cnt -- )      R -) U MOV  R -) 4 MOV
 6      2 S )+ MOV    4 S )+ MOV  ( load data address and count)
 7      U CLR  ( set x coordinate to zero)  4 )+ TST
 8      BEGIN  0 4 )+ MOV  3777 # 0 MUL   77777 # 0 DIV  0DAC 0 MOV
 9        1DAC U MOV     4 )+ TST   U 10 # ADD    2 SOB
10          4 R )+ MOV    U R )+ MOV   NEXT
11 : SCOPE    ( addr cnt -- )
12       #POINTS !  DATA-ADDR !  SCOPE-TASK  ACTIVATE
13           BEGIN  DATA-ADDR @ #POINTS @ 1SCAN   60 MS  0 END ;
14 : SUSPEND  ( task -- )   ACTIVATE  STOP ;          DECIMAL
15
```

```
309 LIST

 0 ( CLOCK INTERRUPT HANDLER TO READ ORTEC 707) BASE @ OCTAL
 1 VARIABLE TICKS/DATUM        ( clock ticks to elapse between data)
 2 VARIABLE ELAPSED-TICKS      ( elapsed tick counter               )
 3
 4 CREATE <PC-EXPECT>   ASSEMBLER
 5
 6   U ' H @ # SUB             ( point to head of user table        )
 7   ELAPSED-TICKS DEC         ( collect data this tick ?           )
 8   0= IF
 9     ELAPSED-TICKS TICKS/DATUM MOV  ( reset tick counter          )
10     R -) S MOV              ( save interrupt user's param stack  )
11     S STATUS 4 + U) MOV     ( get calling user's param stack     )
12     R -) S )+ MOV           ( save calling user's return stack   )
13     R -) S )+ MOV           ( save calling user's instruct ptr   )
14     R -) 0 MOV     -->      ( save all of the registers used     )
15
```

```
310 LIST

 0 ( CLOCK INTERRUPT HANDLER TO READ ORTEC 707 cont.)
 1     R -) 1 MOV              ( ...                                )
 2     R -) 2 MOV              ( ...                                )
 3     R -) 4 MOV              ( ...                                )
 4     2 12 # MOV              ( load radix for number conversion   )
 5     PCSR 1 # BIS            ( initiate the readout sequence      )
 6     BEGIN                   ( wait for "start data transfer"     )
 7       PCSR TST              ( ...                                )
 8     0< END                  ( ...                                )
 9     S -) PCSR 4 + MOV       ( read the most significant digit    )
10     S ) 177760 # BIC        ( mask off bits 4-15                 )
11     S -) CLR                ( make it a double precision integer )
12     4 5 # MOV               ( set up loop cntr for 5 more digits )
13     BEGIN       -->
14     ( convert the incoming BCD digits to a binary number by     )
15     ( multiplying the 32 bit integer on the stack by the radix )
```

```
311 LIST

 0 ( CLOCK INTERRUPT HANDLER TO READ ORTEC 707 cont.)
 1     ( and then adding in the next digit                         )
 2        0 2 S) MOV           ( get low word of developing integer )
 3        2 0 MUL              ( multiply it by ten                 )
 4        2 S) 1 MOV           ( restore low word of product        )
 5        R -) 0 MOV           ( save the high word of product      )
 6        0 S ) MOV            ( get the high word of the integer   )
 7        2 0 MUL              ( multiply it by the radix           )
 8        S ) 1 MOV            ( store low word of this product as  )
 9                             (   high word of developing integer  )
10        S ) R )+ ADD         ( add any carry from the first mult. )
11                             (   into the high word of the integer)
12        S -) PCSR 4 + MOV    ( get next digit from the counter    )
13        S ) 177760 # BIC     ( mask off bits 4-15                 )
14        2 S) S )+ ADD        ( add this digit into the integer    )
15        S ) ADC        -->   ( not to forget the possible carry   )
```

```
312 LIST

 0 ( CLOCK INTERRUPT HANDLER TO READ ORTEC 707 cont.)
 1     4 SOB                  ( got all 6 digits? if not loop back )
 2     PCSR 1 # BIC           ( terminate the readout process       )
 3     4 R )+ MOV             ( restore all registers used          )
 4     2 R )+ MOV             ( restore all registers used          )
 5     1 R )+ MOV             ( ...                                 )
 6     0 R )+ MOV             ( ...                                 )
 7     S -) R )+ MOV          ( resave calling user's IP            )
 8     S -) R )+ MOV          ( resave calling user's return stack  )
 9     STATUS 4 + U) S MOV    ( resave calling user's param stack   )
10     S R )+ MOV             ( restore interrupted users's param   )
11                            (   stack                             )
12                  -->
13
14
15

313 LIST

 0 ( CLOCK INTERRUPT HANDLER TO READ ORTEC 707 cont.)
 1     U ) WAKE # MOV         ( reactivate the calling task         )
 2   THEN
 3   U R )+ MOV               ( restore the interrupted user        )
 4   RTI
 5
 6
 7                                                          -->
 8
 9
10
11
12
13
14
15

314 LIST

 0 ( PHOTON COUNTING DATA AQUISITION TASK)
 1
 2 177560 204 300 TERMINAL PC-TASK       PC-TASK CONSTRUCT
 3     ' <PC-EXPECT> PC-TASK @ 40 + !          0 206 !
 4
 5
 6
 7
 8
 9
10
11
12
13                                                        -->
14
15
```

```
318 LIST

 0 ( EMPTY )
 1
 2
 3
 4
 5
 6
 7
 8
 9
10
11
12
13
14
15
```

```
319 LIST

 0 ( VALVE CONTROL TASK                11/4/83)      BASE @ OCTAL
 1 167760 CONSTANT PCSR               170000 CONSTANT ACLK.CSR
 2 170002 CONSTANT BCLK.CSR           170006 CONSTANT DCLK.CSR
 3 VARIABLE ACLOCK   0 ACLOCK !       VARIABLE VALVES   0 VALVES !
 4 VARIABLE 1VALVE   0 1VALVE !       VARIABLE 2VALVE   0 2VALVE !
 5 VARIABLE DAT-ADDR                  DATA 4 +   DAT-ADDR !
 6
 7 ASSEMBLER    HERE
 8    R -) U MOV   U ACLOCK MOV    CNT U) TST   0< NOT IF   0= IF
 9    PCSR 2+ 1VALVE BIS   THEN   CTR U) DEC   0= IF
10    PCSR 2+ 1VALVE BIC   ACLK.CSR CLR   VALVES DEC   0= IF
11    ACLOCK I) WAKE # MOV   THEN   THEN   THEN
12    CNT U) INC   U R )+ MOV   200 200 INTERRUPT
13
14                                                 BASE !  -->
15
```

```
320 LIST

 0 ( VALVE CONTROL TASK                12/7/83)      BASE @ OCTAL
 1
 2 VARIABLE D.CNT  0 D.CNT !        VARIABLE D.CNTR  0 D.CNTR !
 3
 4 ASSEMBLER    HERE
 5    D.CNT TST   0< NOT IF   0= IF
 6    PCSR 2+ 2VALVE BIS   THEN   D.CNTR DEC   0= IF
 7    PCSR 2+ 2VALVE BIC   DCLK.CSR CLR   VALVES DEC   0= IF
 8    ACLOCK I) WAKE # MOV   THEN   THEN   THEN
 9    D.CNT INC   PCSR 2+ 2000 # BIS   PCSR 2+ 2000 # BIC
10                                        200 350 INTERRUPT
11
12                                                 BASE !  -->
13
14
15
```

```
321 LIST

 0 ( VALVE CONTROL TASK                12/6/83)          OCTAL
 1
 2 CODE (VALVE-ON)    ( valve.mask.1 open.time.1 valve.mask.2
 3                      open.time.2  -- )
 4    D.CNTR S )+ MOV    D.CNT -2 # MOV    2VALVE S )+ MOV
 5    0= NOT IF    VALVES INC    DCLK.CSR 103 # MOV    PCSR 100 # BIS
 6    THEN     CTR U) S )+ MOV    CNT U) -1 # MOV    1VALVE S )+ MOV
 7    VALVES INC     ACLK.CSR 103 # MOV      WAIT JMP       DECIMAL
 8
 9 : VALVE-ON    ACLOCK GET  (VALVE-ON)    ACLOCK RELEASE ;
10
11 : MIX      ( -- )     1  1300    2  800     VALVE-ON ;
12 : INJECT   ( -- )     4   800    0    0     VALVE-ON ;
13 : FILL     ( -- )    16   800    0    0     VALVE-ON ;
14 : WASH     ( -- )     1   900    0    0     VALVE-ON ;
15                                                      -->

322 LIST

 0 ( VALVE CONTROL TASK                12/6/83)
 1
 2 : DRAIN    ( -- )
 3      128 PCSR 2+ !     200 MS      192 PCSR 2+ !     200 MS
 4      448 PCSR 2+ !    2000 MS      192 PCSR 2+ !     500 MS
 5       64 PCSR 2+ !     500 MS        0 PCSR 2+ ! ;
 6
 7
 8 OCTAL
 9 177560  160  400  TERMINAL VALVE-TASK      VALVE-TASK CONSTRUCT
10                                                DECIMAL
11
12
13
14
15                                                      -->

323 LIST

 0 ( VALVE CONTROL TASK                12/7/83)
 1
 2 : RINSE    ( -- )  DRAIN    FILL  500 MS  WASH  1000 MS  DRAIN
 3      1000 MS  WASH    1000 MS  DRAIN  1000 MS DRAIN ;
 4
 5 : LOAD-POSN   ( -- )  VALVE-TASK ACTIVATE  INJECT  STOP ;
 6
 7 : INJECT-MARK   ( -- )  DAT-ADDR @ 4 -  DUP  2@   2DUP  D+
 8      ROT 2! ;
 9
10 : INJECT-SAMPLE   ( -- )    VALVE-TASK ACTIVATE
11      INJECT-MARK    MIX    STOP ;
12
13
14 : RINSE-CELL   ( -- )    VALVE-TASK ACTIVATE  RINSE  STOP ;
15
```

```
324 LIST

 0 ( EMPTY )
 1
 2
 3
 4
 5
 6
 7
 8
 9
10
11
12
13
14
15


325 LIST

 0 ( PEAK INTEGRATION TEST STUFF)
 1 292 LOAD ( STATS STUFF)
 2
 3 2VARIABLE TAREA                    2VARIABLE BASELINE
 4 2VARIABLE HEIGHT
 5
 6 : HEIGHTS  ( addr -- )   0. TAREA 2!  0. HEIGHT 2!
 7         DUP 50 MEAN  BASELINE 2!
 8         DUP 992 +  SWAP  224 + DO  I 2@  BASELINE 2@ F-
 9         2DUP  TAREA F+!  HEIGHT 2@  FMAX  HEIGHT 2!  4 +LOOP
10        ." Area ="  TAREA 2@  E.  ."  Height ="  HEIGHT 2@ E. ;
11
12 : PSHOW  ( sblk# dblk# -- )
13         1+ SWAP DO  CR I DUP 3 U.R 2 SPACES  BLOCK AREA LOOP ;
14
15


326 LIST

 0 ( EMPTY )
 1
 2
 3
 4
 5
 6
 7
 8
 9
10
11
12
13
14
15
```

The vita has been removed from the scanned document

THE DESIGN AN APPLICATION OF AN AUTOMATED LUMINOMETER FOR CHEMILUMINESCENCE

by

Ian Chapple

(Abstract)

An automated luminometer was designed and constructed to facilitate the investigation of reaction conditions and quantitation of the chemiluminescence observed during the oxidation of NADH by horse radish peroxidase in the presence of eosin.

The luminometer design incorporates a computer controlled reagent induction system, pulse counting detector and real time display of luminescence profiles.

Each of the major reaction conditions was studied individually to determine the most favorable conditions for the analytical application of this reaction. In addition, this chemiluminescent reaction was studied to determine if the luminescing species is recycled. If this were the case it would provide the first essential step necessary for the future design of a chemiluminescent probe that could be reuseable or be used for continuous monitoring.

During the course of this investigation it was observed that the luminescing species, eosin, was being

bleached. A number of experiments were undertaken to determine the nature of the bleaching process. Those steps which suppressed the bleaching process, unfortunately, also suppressed the emission process.

Despite the fact that this reaction does not appear to recycle the luminescing species, it does provide a chemiluminescent method for the determination of NADH over the range $5x10^{-6}$M to $5x10^{-4}$M. This chemiluminescent reaction has also been coupled to several enzyme systems, which reduce NAD^+ to NADH, in order to obtain a chemiluminescent signal proportional to the substrate concentration.